CBS LABORATORIES

FINAL REPORT

SHORT WIDE ANGLE, 1-1/2 INCH ELECTROSTATIC IMAGE DISSECTOR WITH PARALLEL PLATE RESISTIVE STRIP ELECTRONIC MULTIPLIER

Period Covered: 22 February 1963 to 1 November 1965

Project No.: 5237

Date: 1 December 1965

Prepared For: Jet Propulsion Laboratory
California Institute of Technology
Pasadena, California

Prepared By: J. Karpinski
J. Karpinski
Tube Engineer

Approved By: Charles F. Misso
C.E.F. Misso, Section Head, Electron Tube Dept.
CBS Laboratories, A Division of Columbia Broadcasting System, Inc.
Stamford, Connecticut

Contract No. 950508

"This work was performed for the Jet Propulsion Laboratory, California Institute of Technology, pursuant to a sub-contract issued under Prime Contract NAS7-100 between the California Institute of Technology and the United States of America represented by the National Aeronautics and Space Administration."

CONTENTS

Page

1. INTRODUCTION 1

2. THE IMAGE SECTION 3

2.1 Image Section Electron Optical Study . . . 3

2.2 The Two Electrode Electron Optical Imaging System 5

2.3 Faceplate Mounting Design 6

3. THE INTEGRATED ANODE-DEFLECTION CONE 7

4. FABRICATION OF EXPERIMENTAL TUBES 9

5. EXHAUST AND TEST RESULTS 10

5.1 Deflection Plate and Aperture Alignment . 10

5.2 The Electronic Spot Size 10

5.3 Deflection Evaluation 11

5.4 General 12

6. CONCLUSIONS 14

APPENDIX I

ILLUSTRATIONS

Fig. 1 Faceplate Mounting (Previous Design)

Fig. 2 New Faceplate Mounting

Fig. 3 Image Section Electrostatic Field Plots

Fig. 4 Focus Electrodes

Fig. 5 Electron Optical System Consisting of Concentric Spheres

Fig. 6 Electron Optical System Consisting of Concentric Spheres with Hole in the Anode

Fig. 7 Anode Deflection Cones

Fig. 8 Electronic Spot Size Vs. Displacement at Photocathode

Fig. 9 Image Section Distortion

1. INTRODUCTION

The purpose of this program was to design and develop a short wide angle 1 1/2" diameter electrostatic image dissector with a parallel plate resistive strip electron multiplier and an integrated drift free anode/deflection system. The development of a parallel plate resistive strip electron multiplier was prompted by the anticipated reduction in length, weight and associated circuitry. The work undertaken to achieve these goals was divided into three phases.

In the first phase the feasibility of making a practical electrostatic resistive strip electron multiplier within a device was demonstrated. During this work it became evident that serious limitations existed which prevented the manufacture of a small high gain strip multiplier capable of handling relatively high input currents. Devices were made with gains in the order of 10^5 however, it was found that material limitations would not permit the design objectives to be achieved. For these reasons it was recommended that future effort be directed toward the design and development of miniaturized electron multipliers using conventional secondary emissive surfaces and multiple electrodes.

The second phase was devoted to

(1) a study of the image section electron optics in an effort to extend the useful field and improve the electron optical resolution.

(2) The redesigning of the input faceplate mounting to improve the electric field uniformity near the peripheral areas

of the photocathode and to permit the use of a rugged vacuum deposited cathode connection.

(3) The design and development of an integrated anode cone and a high linearity no drift deflection system.

The developments resulting from work in each of these three areas were incorporated in prototype devices made in the third phase of the program. Significant improvements in resolution, from the center to the edge of the photocathode and the complete absence of drift in the new deflection system were observed in the evaluation of the prototype tubes.

This report covers the work performed during the second and third phases of the program. The work conducted in the first phase was the subject of the Interim Engineering Report dated November 1964, attached as Appendix I of this report.

2. THE IMAGE SECTION

2.1 Image Section Electron Optical Study

A limited study of the electron optics of the image section was undertaken in an effort to generate a design which would improve the overall resolution of the image dissector. The study was performed with the aid of electric field plots made with resistive paper analogues. Although these in themselves have limited use when applied to the initial design of three dimensional electron optical systems they do have a significant value in the study of variations of an existing design.

True scale (20x) replicas of the diametrical cross sections of the image section electrode configuration were drawn using highly conductive paint on Teledeltos resistive paper. Appropriate potentials from a well regulated D.C. supply were applied to the electrodes. The equipotential lines were plotted using a potentiometer and a null indicator. Initially field plots of the existing design with and without the modified faceplate mounting, were made.

Figures 1 and 2 illustrate the two faceplate sub-assembly designs. The modification resulted in an improvement in the field uniformity across the photocathode.

The effect of increasing the smaller diameter of the focus electrode was then studied. An increase of 0.1 inches improved, to some extent, the uniformity of the electric field shape in the fringe areas however, further improvement was still desirable. At this time consideration was given to modifying the envelope in order to accommodate a focus

electrode 0.2 inches larger in diameter then the earlier design. This resulted in the development of the image section design shown in Figure 3(b). Figure 3(a) shows the earlier design with the modified faceplate contour.

In order to obtain some measure of the electric field uniformity a summation of the radii of field line curvatures was performed along the tube axis and along the lines normal to the photocathode surface at 0.4 inches from the axis.

The numerical results are shown below.

Summation of Curvatures,

	Fig. 3(a) Standard Design	Fig. 3(b) Modified Design
$\sum \frac{1}{r}$ along axis	.04506	.05327
$\sum \frac{1}{r}$ 0.4" from axis	.04905	.05146
Difference	.00399	.00181
Percentage difference	8%	4%

It is evident that the value of $\sum \frac{1}{r}$ is more uniform in the modified design and therefore a greater uniformity of focus would be expected. This is so because in a theoretical, two element spherical electron optical system the value of $\sum \frac{1}{r}$ is the same for electrons emitted from all points of the photocathode. Because of inaccuracies in the experimental methods and variations in the resistive paper direct comparisons of the equipotential lines of the two designs should not be made. However, it can be seen that the numerical difference

between $\lesssim \frac{1}{r}$ of the two designs is small. In practice this would be compensated by a fractional difference in focus electrode potential. Both the old and the new focus electrodes are shown in Figure 4.

Electric field plots of the earlier design with flat or spherical grids at the apex of the anode cone demonstrated that these had a negligible effect on the field shape near the photocathode. The use of the grids was not considered further since their use would have radically changed the focal length of the electron optical system. This is evident when the dimensions of the electron optical system components are substituted in the theoretical model equations (1) and (2) of Section 2.2.

2.2 The Two Electrode Electron Optical Imaging System

Since the electron optical design of the image dissector is a modified form of the two electrode model using two concentric spheres, the theory of this model was considered during the image section electron optical study.

Figure 5 shows the first model of two concentric spherical electrodes in which the inner surface of the larger sphere is considered as the cathode and the outer surface of the smaller as the anode. In this model a virtual image of the cathode is formed on a spherical surface of radius R, where $Ri = \frac{n}{n-2} Ra$ — — — — — — (1)

$n = \frac{Rc}{Ra}$, and

Rc = radius of photocathode

R_a = radius of the anode

The electron optical system shown in Figure 6 is similar except for the hole in the anode, the smaller sphere. In this model a real image is obtained however the divergent or negative lens action of the hole results in a considerable increase in the focal length. The image of the cathode in this electron optical system is located on a spherical surface of radius Ri where

$$Ri = \frac{6\,(n-1)}{n-4}\,Ra \qquad (2)$$

2.3 Faceplate Mounting Design

The object of the work undertaken in this area was to overcome the re-entrant condition at the periphery of the photocathode. This was necessary to improve electric field uniformity and to eliminate the need of using conductive paint to provide an electrical connection to the photocathode. Figure 1 shows the earlier design in which the above improvements were required.

After preliminary faceplate sealing experiments the design shown in Figure 2 was generated. In this design the center of the faceplate is accurately aligned with the subassembly by a small step at the inner edge of the plate. Besides assuring good axial alignment of the faceplate the design minimizes the surface area of the frit material exposed to the interior of the tube; it also permits the use of a rugged, vacuum deposited aluminum cathode connection. Since both the silver paint and frit material have an afinity and gettering action on the alkali metals the design changes should enhance the long term stability of the tube.

3. THE INTEGRATED ANODE-DEFLECTION CONE

The purpose of the work undertaken in this phase of the program was to develop an integrated anode deflection cone with an extremely stable drift free deflection system which would be accurately aligned with the electron optical imaging system. Prior to the development discussed, the deflection elements of the deflectron deflection system were deposited on an insulating substrate which was in the same plane as the elements. Photoelectrons landing on the insulation between the deflection elements caused spurious charging effects which resulted in deflectron instability; this is generally termed hysteresis or drift. In practice when the tube is used in a guidance system such as a star tracker, this would be evident by an apparent change in position of the star.

To fulfill the technical requirements the development of a precision ceramic-metal anode/deflection cone assembly, with deflection elements mounted above the ceramic surface, was undertaken.

Initially, forming the deflectron plates by selective etching techniques out of a spun bi-metal cone was considered. However, this was abandoned because of variations in the thickness of the metal and the difficulty in maintaining sufficiently close tolerances.

After further study an integrated anode/deflection cone of the type shown in Figure 7 was developed. In this design the deflectron elements are formed by selective etching of a hollow metal cone. The wall thickness of the cone is machined to close tolerances to facilitate the establishment of weld schedules for attaching the deflectron elements

to short nickel pins (6 per element) previously brazed into the ceramic cone. Prior to the welding, the nickel pins are machined to close tolerance in order to ensure perfect matching with the deflection elements.

The metalized portion of the apex of the ceramic cone, as shown in Figure 7 performs the function of the metal anode cone used in the original design. The interior of the hole at the apex is also metalized to prevent spurious charging effects. Two metallized strips provide electrical connections to the Kovar base which is used to mount the assembly within the tube.

4. FABRICATION OF EXPERIMENTAL TUBES

Thirteen tubes incorporating the integrated anode/deflection cone, the new focus electrode and the modified faceplate mounting were assembled under this program. Two of these numbers M1301 and M1304 were not exhausted because of leaks found in the faceplate frit seal. The leaks developed during the post aluminization bake of the front end assemblies. The dark color of the frit in these seals led to the belief that the drying out process was not completed before the high temperature bake. Since there was no change in the bake cycle an increase in concentration of the frit suspension vehicle was suspected. Thinning of the vehicle and the added precaution of increasing the drying time prevented reoccurrance of this problem.

In order to accommodate the increased diameter focus electrode suitable modifications were made to the front end of the tube.

New and additional fixtures were made as required by the new components.

Throughout the program weld schedules were developed as required and all new processing techniques were established as new specifications.

During the program comprehensive design and process records were kept. Quality assurance was performed as an engineering function and the necessary standards, required to perform this type of work, were maintained. This approach was followed in order to minimize the difficulties which can occur in the transferring of the developmental ideas and processes into a program requiring the rigorous quality assurance procedures associated with flight hardware.

5. EXHAUST AND TEST RESULTS

Eleven tubes were exhausted during the program and of these five were fully tested. The tests of the remaining six tubes were discontinued due to various reasons listed in Table I.

5.1 Deflection Plate and Aperture Alignment

After the assembly of the first four tubes with deflectrons aligned according to indexing marks it was found that there was a consistent 8-9° misalignment. When this was determined a suitable correction factor was applied to subsequent tubes. After determination and application of the correction factor the alignment in all tubes was within 2°.

5.2 The Electronic Spot Size

The electronic spot size measurements were made according to the following method. With the image section potential of 700 volts and the focus electrode voltage adjusted for maximum resolution at the center of the photocathode a small circular spot of light (.001" diameter) was focused on the photocathode and moved along the horizontal, vertical and diagonal diameters of the photocathode up to .4 inches away from the tube axis. Because of the plano-concave shape of the faceplate the spot was refocused optically at every point on the photocathode where spot size measurements were made. At each of these points the spot was moved across the aperture until the anode output decreased to 20% of its maximum value. The distance between the 20% amplitude points less the effective aperture width or length, depending whether the spot was moved

TABLE I

Tube Serial Number	Photocathode Sensitivity μA/L	Gain at 125V/Stage	Anode Dark Current μA	Misalignment Degrees	Uniformity		Deflection Sensitivity * Inch/Volt	Overall Response %
					Cathode .1" Spot %	Dynode %		
M1288	—	Tube Broke off Pump During Bake				Deflectron Cone Reclaimed		
M1289	26.2	$2x10^8$	.05	8	65.5	95.5	.00155	32
M1290	104	$5.9x10^7$	.062	9	76	94	.00178	76
M1291	84.5	$8.4x10^7$	.06	8	81	68	Low Sensitivity Area In Center Of Photocathode	
M1292	86.5	Tube Cracked at Test			85	—	—	—
M1293	50.0	$3.0x10^7$	.025	—	90	Open Deflection Plate Deflectron Cone Reclaimed		
M1294	68.0	$4.7x10^7$	.24	1.0	67	96	.00187	54.5
M1295	7.0	Low Photocathode Sensitivity				Deflectron Cone Reclaimed		
M1300	65	$6.9x10^6$	.007	2.0	93.5	78.5	.00185	83
M1303	30	Ion Spot			75	—	—	—
M1305	56	$9.7x10^7$	.017	.5	85	80	.00185	62

*Measured With 700 Volts Applied Across the Image Section

CBS LABORATORIES

vertically or horizontally, was taken as the spot diameter. The measurements were made for both vertical and horizontal diameters in order to determine the shape of the spot. According to the measurements the spot remained circular in shape at up to 0.4 inches from the center of the photocathode. The curves of Figure 8 show the variations in electronic spot size as a function of displacement from the center of the photocathode. The increase in spot size from the center of the photocathode to 0.2 inches from the center was very small. Thereafter the rate of spot size growth increased. Referring to Figure 8 it is worthwhile comparing the performance of the tubes made in this program with that of tubes numbers M1108 and M1109 which were made according to the previous design. Similar faceplates and mountings were used in both types.

5.3 Deflectron Evaluation

Drift tests were made of experimental tubes falling from 65°C to room temperature. In no case was there drift or deflection hysteresis observed in any of the image dissectors incorporating the new integrated anode/deflection cone.

The interelectrode leakage resistance of the integrated anode/deflection cone was in excess of 500 megohms in every tube tested. This compared favorably with the maximum of 30 megohms specified on tubes previously developed.

The linearity of the new deflection system was within 1% along the x and y axes. Limitations in the test equipment and the increasing

spot size near the edge of the photocathode prevented a more precise evaluation.

Figure 9 illustrates the typical format of the pincushion distortion which occurred in the image sections. This type of distortion is characteristic of electrostatically focussed imaging systems. The degree displayed does not suggest that the distortion introduced by the deflectron was a major factor.

5.4 General

All tubes were constructed and processed according to specified procedures. In order to minimize the residual gas pressure each tube was exhausted with an auxiliary ion pump which was sealed off after post exhaust ageing.

The average photocathode sensitivity of the tubes exhausted successfully in this program was 65 microamperes per lumen. This compares favorably with the average sensitivity of 46 microamperes per lumen for tubes delivered under JPL Contract No. 950848. The latter figure includes a correction factor to account for the absorption of the fiber optic faceplate.

An increase in the electron multiplier gain was also obtained. The average and minimum gain figures of tubes made during this program were approximately three times greater than those of tubes made in the earlier program.

The above improvements can be attributed to the elimination of the conductive silver paint and its residual contaminants in the cathode contact and deflectron in addition to continual development

of process and exhaust controls.

Gas pressure monitoring, with the auxiliary ion pumps during ageing, indicated that there was a significant reduction in the amount of gas evolved during this process. This and the improvement in the photo and secondary emissive surfaces indicates that significant advances have been made in the tube design and processing.

6. CONCLUSIONS

An improved 1 1/2" diameter image dissector was developed.

Limited electron optical studies led to the generation of an image section design with greatly improved electronic resolution.

Efforts directed at developing a rugged precision, drift free, integrated anode deflection cone were completely successful.

A number of tubes incorporating the new electron optical design and the integrated anode deflection cone were made. No evidence of spurious charging effects which cause small uncontrolled excursions of the electronic image was detected in any of the tubes tested.

The continuing development of process and exhaust techniques in addition to the elimination of the conductive paint, previously used for internal cathode connection resulted in a substantial improvements of photo and secondary emissive surface performance.

The studies performed and the results obtained in this program lead us to conclude that further improvement can be achieved in the electron optical resolution of the image dissector tube.

It is recommended that future work should include a study and the redesigning of the deflectron in order to increase the deflection sensitivity and to reduce the effect of its associated fields on the electronic spot size. This work should include an experimental study to determine the deflectron electrode modification necessary to correct the pincushion distortion which is inherent in the electrostatic electron optical imaging system.

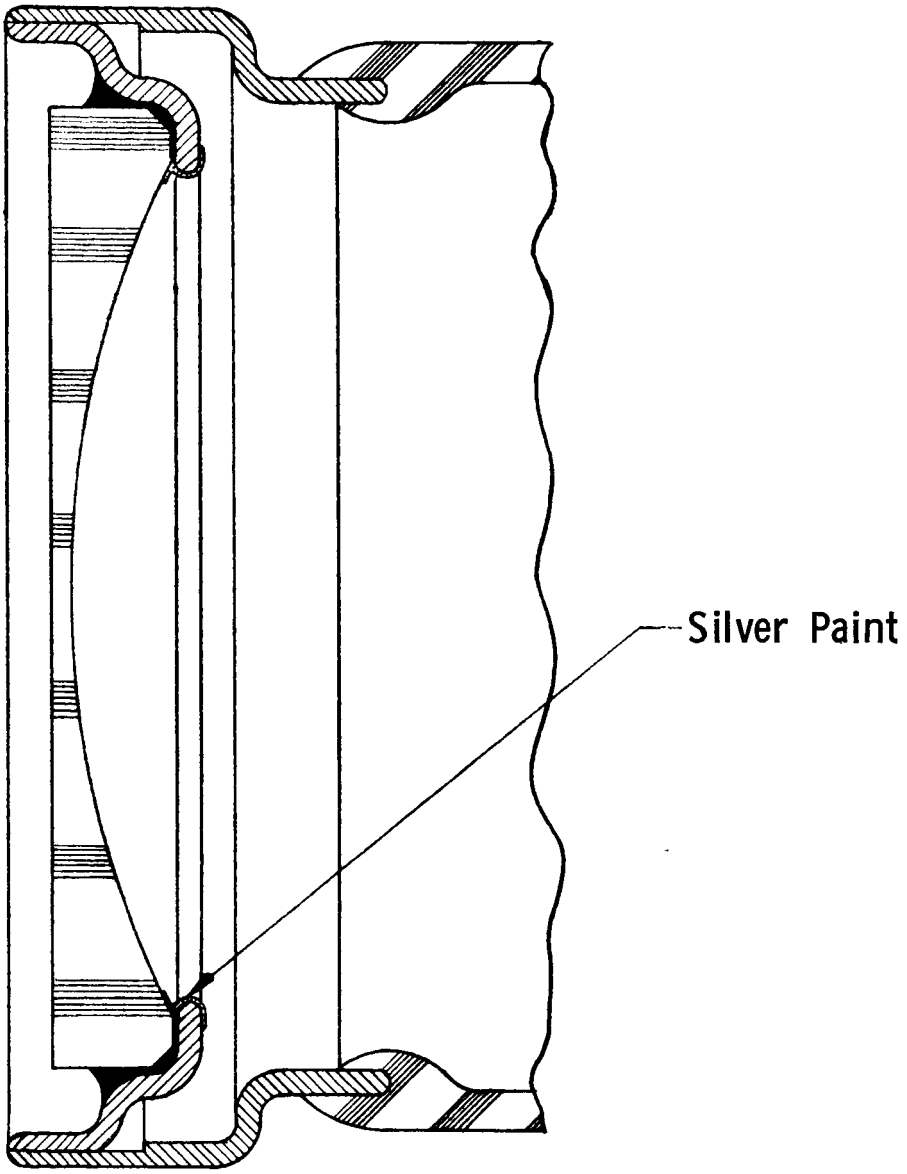

FACEPLATE MOUNTING (Previous Design)

FIG. 1

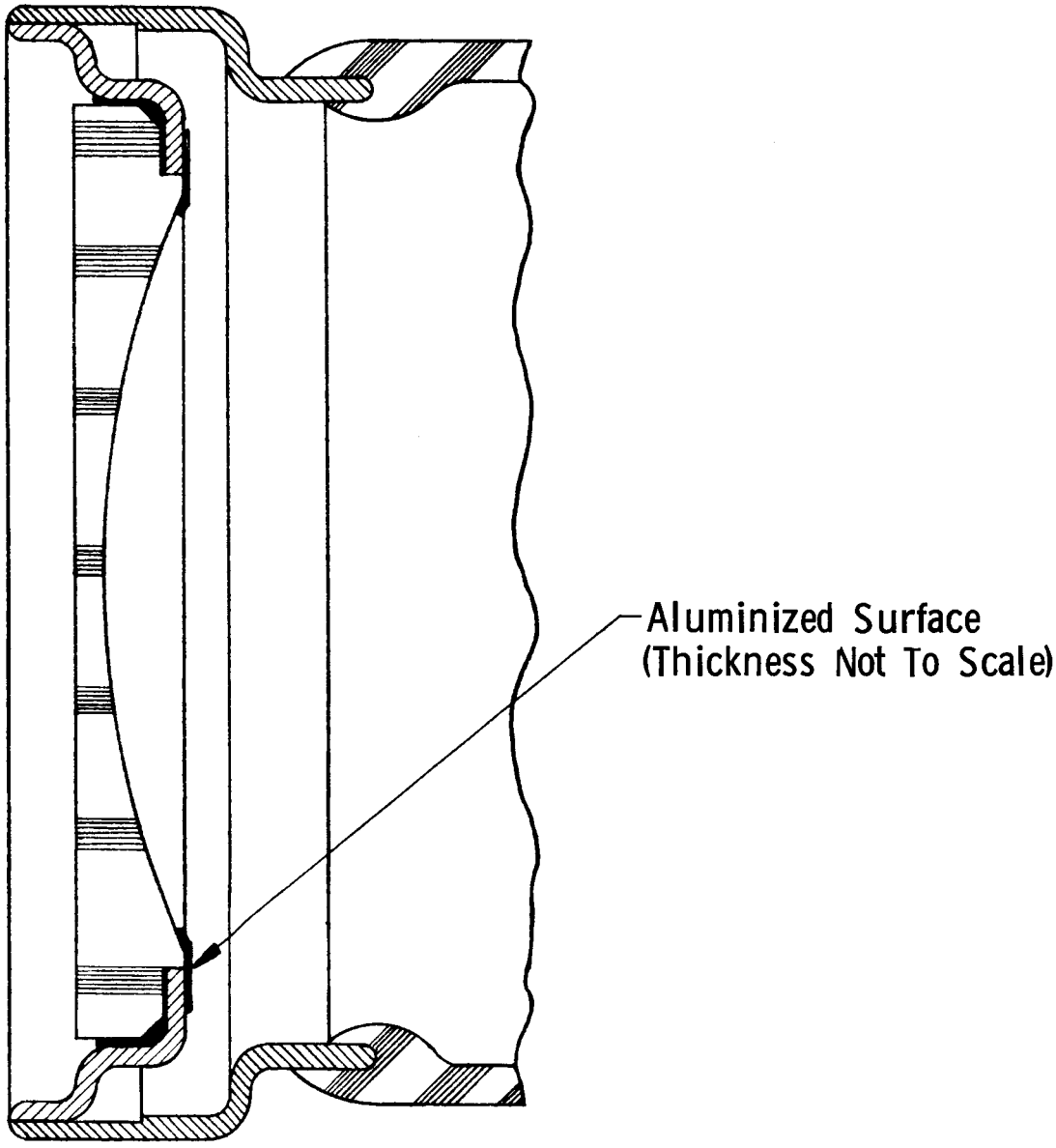

FACEPLATE MOUNTING (New Design)
FIG. 2

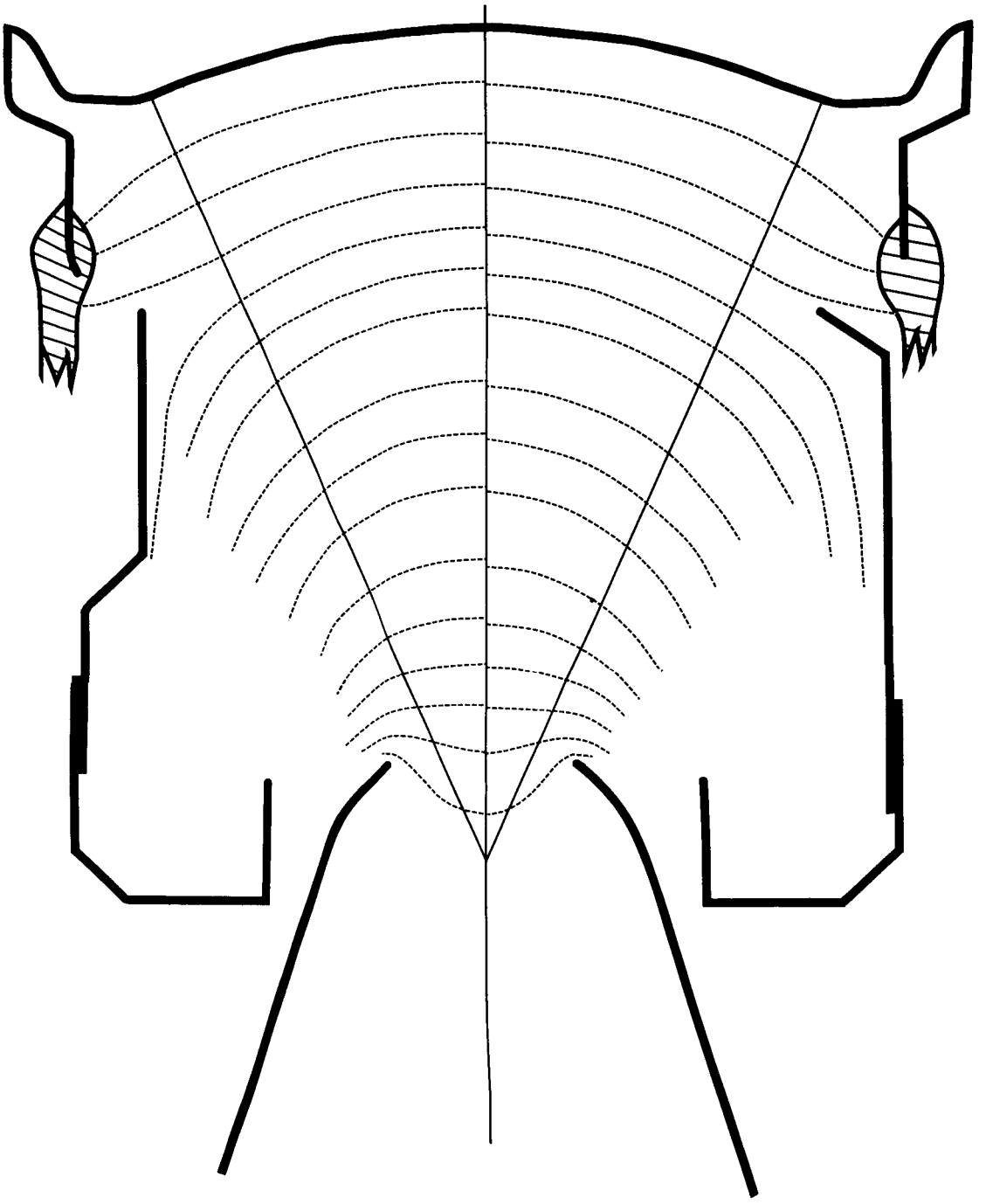

IMAGE SECTION ELECTROSTATIC FIELD PLOTS
FIG. 3

Previous Design

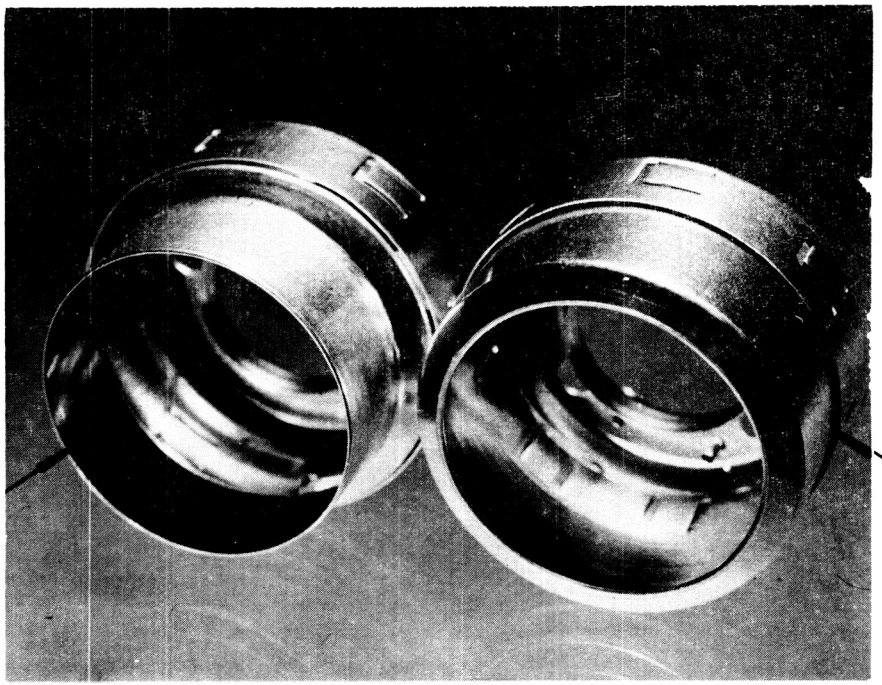

New Design

FOCUS ELECTRODES
FIG. 4

CBS LABORATORIES

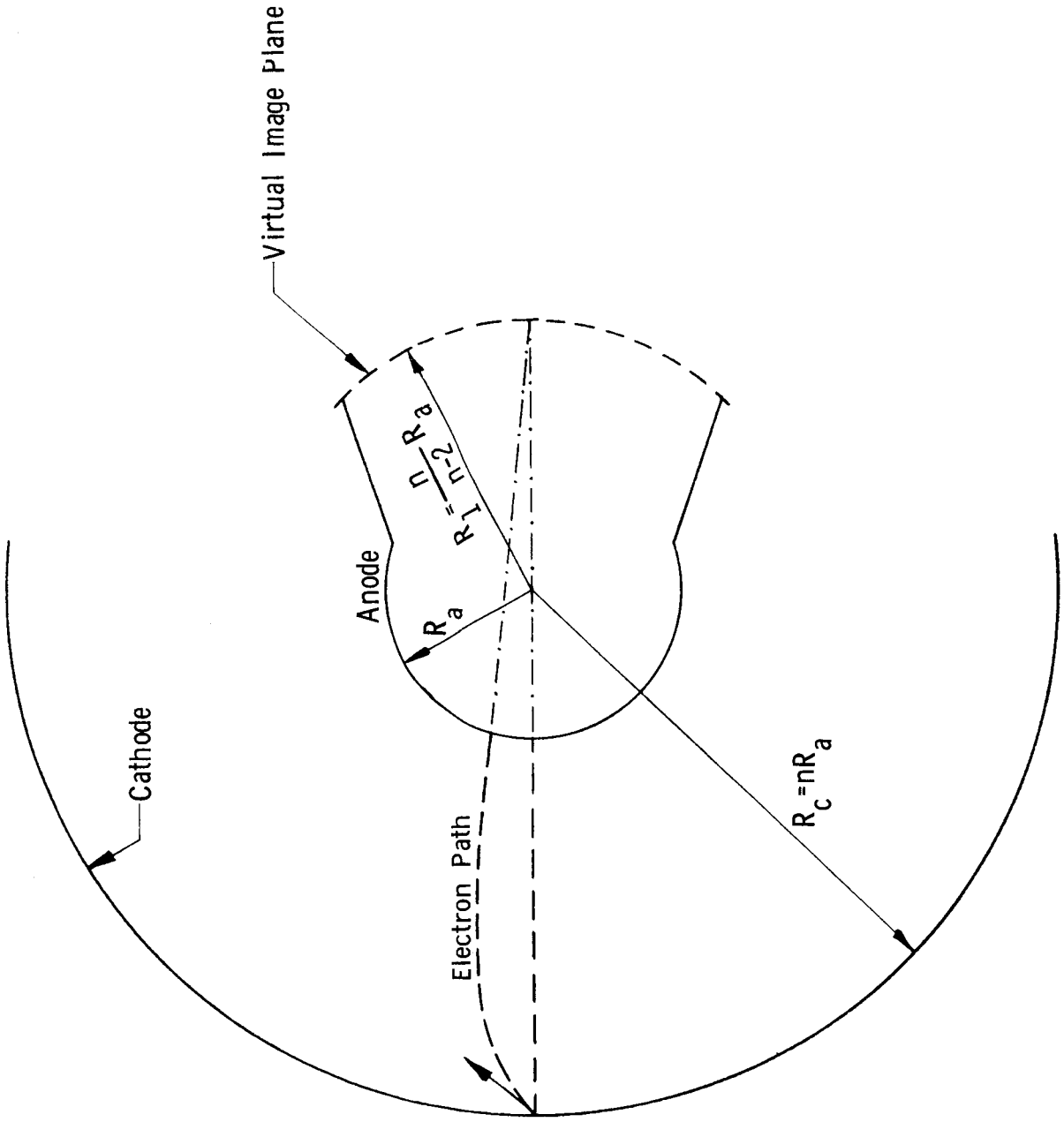

ELECTRON OPTICAL SYSTEM CONSISTING OF CONCENTRIC SPHERES

FIG. 5

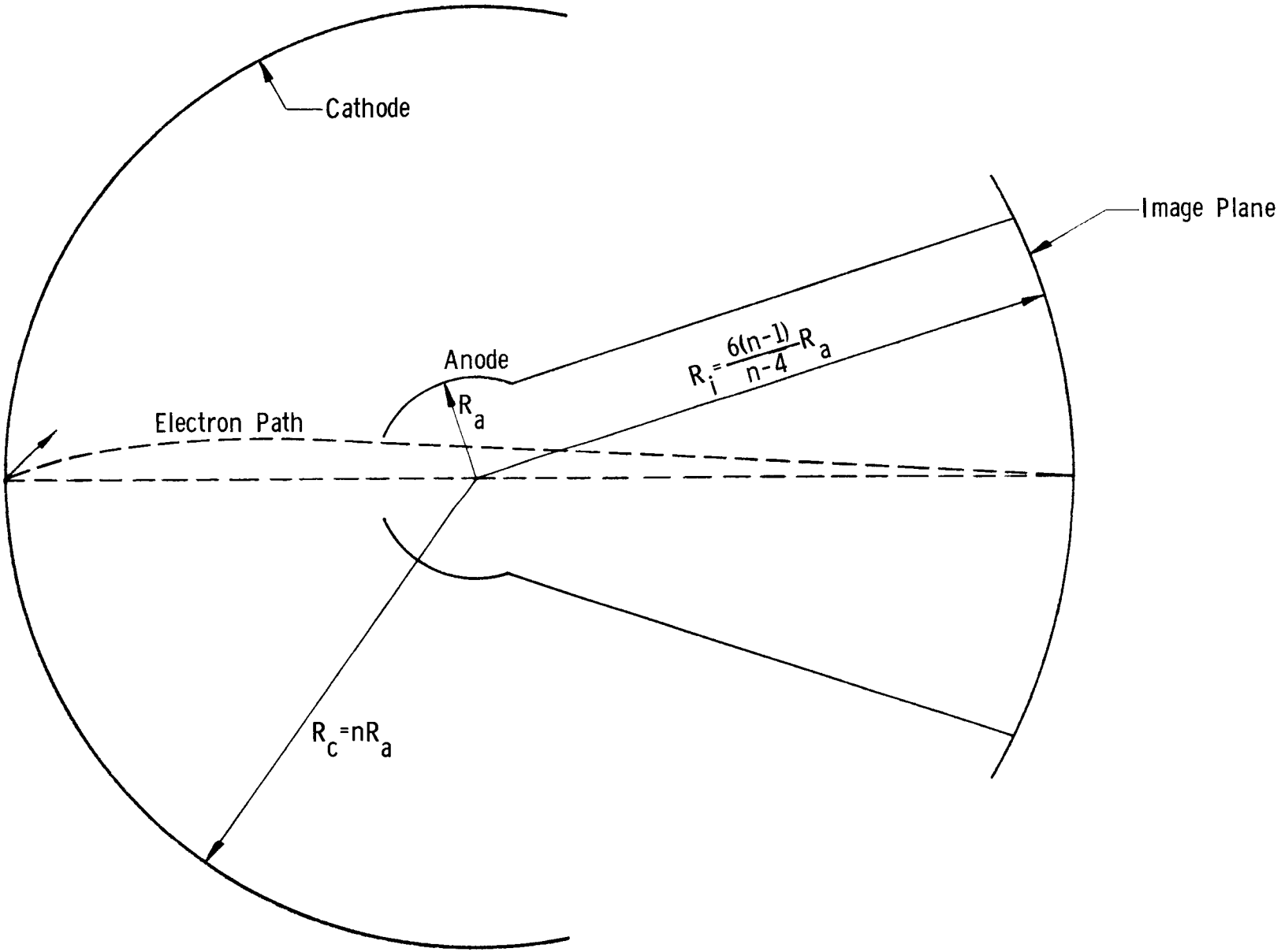

ELECTRON-OPTICAL SYSTEM CONSISTING OF CONCENTRIC SPHERES
WITH HOLE IN THE ANODE

FIG. 6

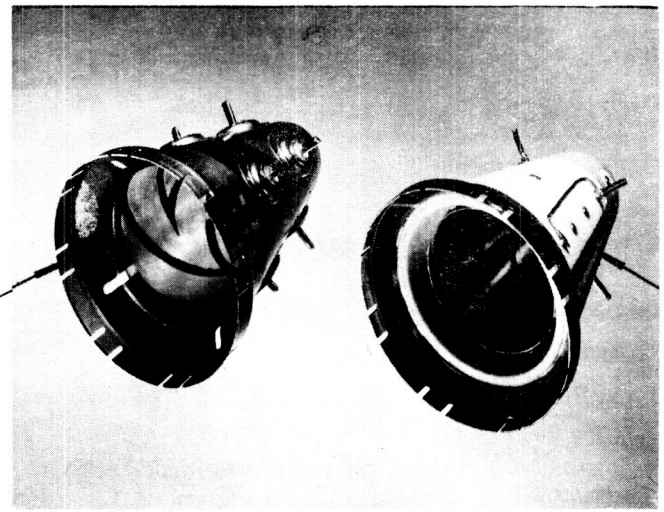

ANODE/DEFLECTION CONES

FIG. 7

CBS LABORATORIES

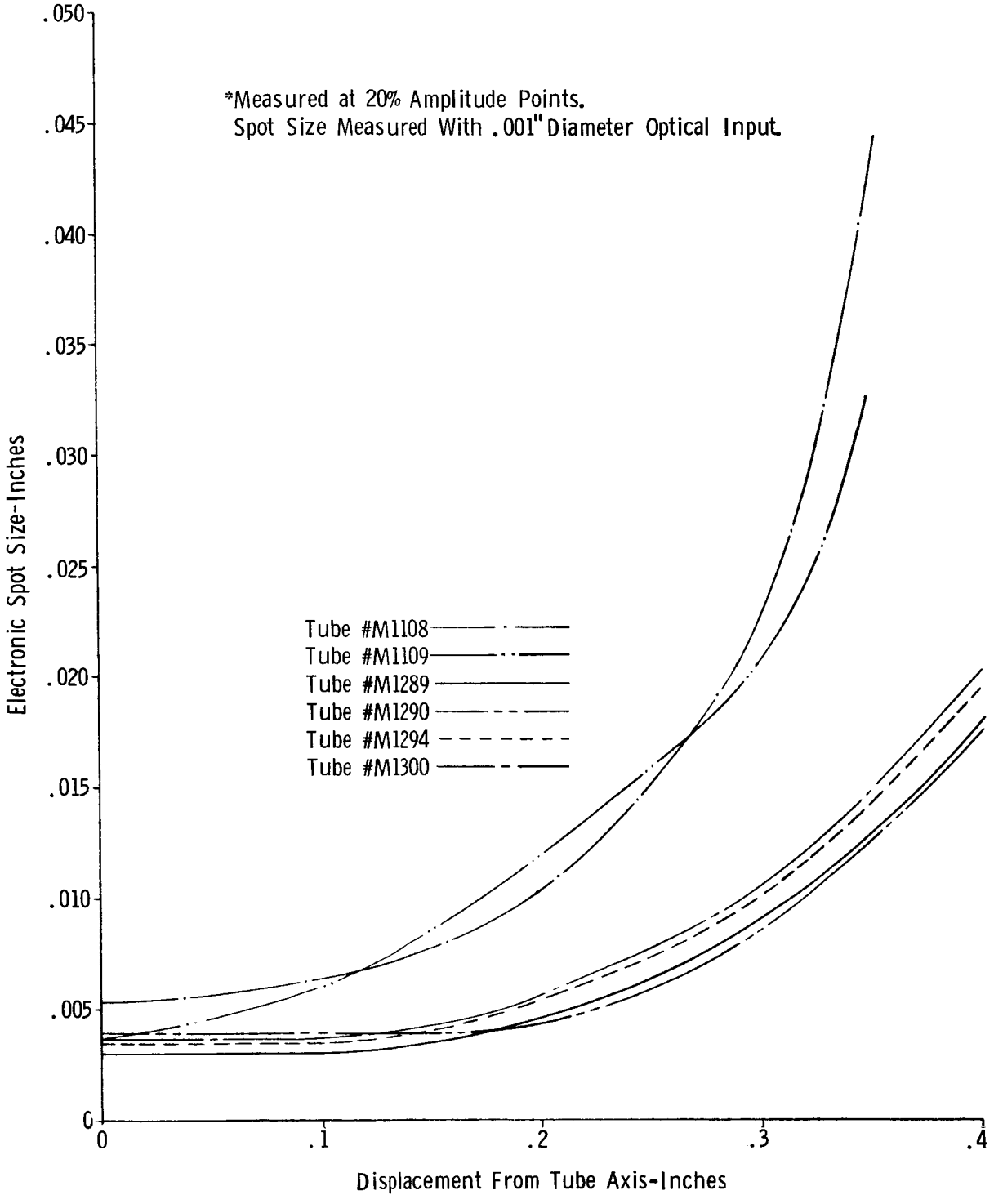

ELECTRONIC SPOT * SIZE vs DISPLACEMENT AT PHOTOCATHODE

FIG. 8

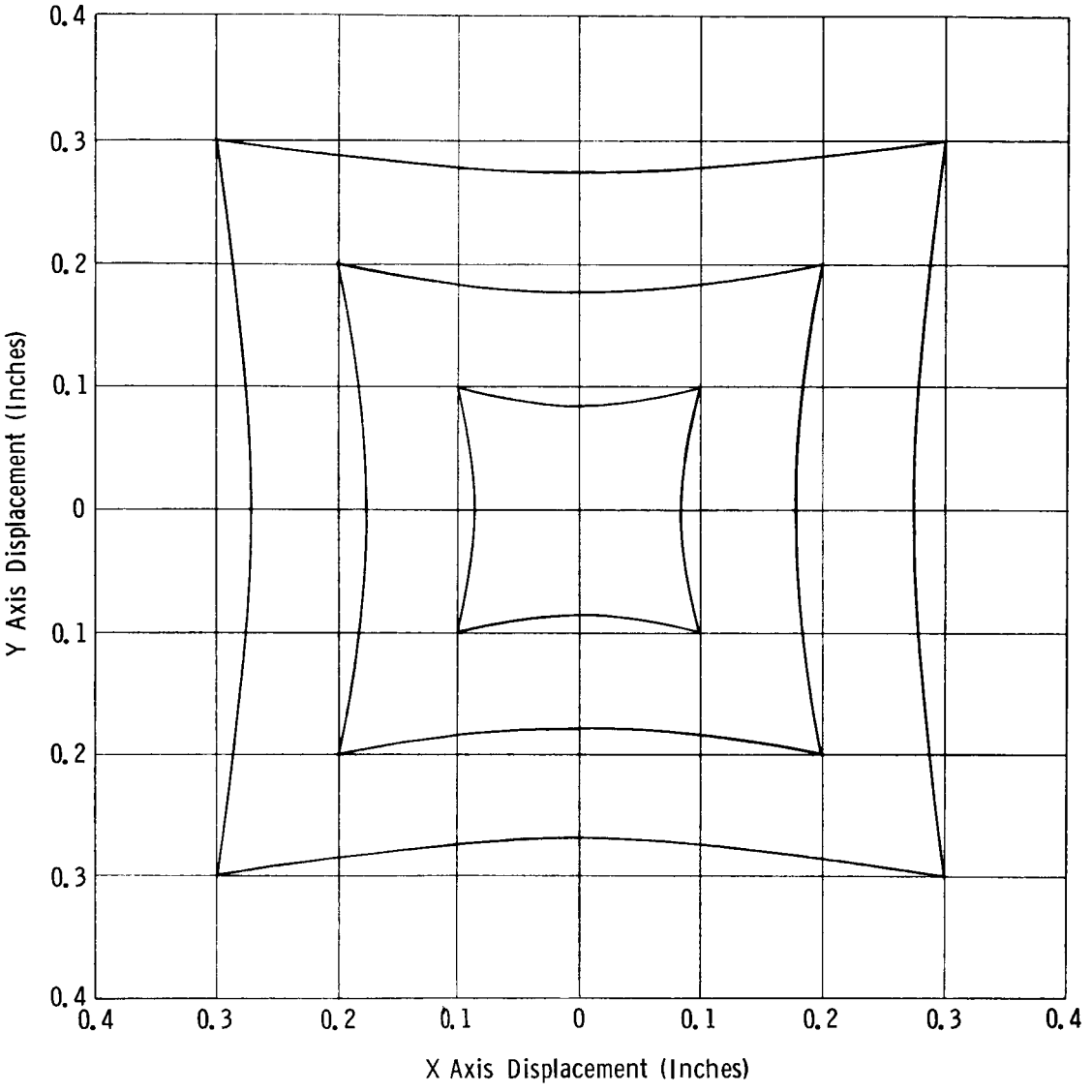

IMAGE SECTION DISTORTION
FIG. 9

APPENDIX I

CBS LABORATORIES

Contract No. 950508

INTERIM ENGINEERING REPORT

SHORT WIDE ANGLE, 1-1/2 INCH ELECTROSTATIC IMAGE DISSECTOR WITH PARALLEL PLATE RESISTIVE STRIP ELECTRONIC MULTIPLIER

Period Covered: 22 February 1963 to 29 February 1964

Project No.: 5237

Date: November 10, 1964

Prepared For: Jet Propulsion Laboratory
California Institute of
Technology
Pasadena, California

Prepared By: Jerry Karpinski
J. Karpinski
Tube Engineer

Approved By: Charles E. F. Misso
C. E. F. Misso, Section
Head, Electron Tube Dept.
CBS Laboratories, A
Division of Columbia
Broadcasting System, Inc.,
Stamford, Connecticut

CONTENTS

		Page
1.	INTRODUCTION	1
2.	THEORETICAL CALCULATIONS	3
3.	RESISTIVE STRIP DEVELOPMENT	9
4.	EXPERIMENTAL TUBE DEVELOPMENT	11
5.	EXPERIMENTAL TUBES TESTS AND DISCUSSION	13
6.	PARALLEL FIELD EXPERIMENTS	16
7.	CONCLUSIONS	20
8.	REFERENCES	21

ILLUSTRATIONS

1. Multiplier Strip in Parallel Electric Field

2. Design of Ladder Type Nichrome Film Multiplier Strip

3. Schematic of Experimental Strip Multiplier Tube

4. Effective Strip Conduction Current Vs. Applied Voltage (First Experimental Strip Multiplier)

5. Strip Multiplier Gain Vs. Applied Voltage (First Experimental Strip Multiplier)

6. Multiplier Gain Vs. Applied Voltage (First Experimental Strip Multiplier)

7. Strip Multiplier Gain Vs. Applied Voltage - Grid Potential Adjusted For Maximum Gain (Second Experimental Strip Multiplier)

8. Schematic of Experimental Strip Multiplier Tube

9. Electron Multiplier Gain (Multiple Grid Design)

10. Schematic of Parallel Electric Field Experiment

11. Multiplier Strip Gain Vs. Applied Voltage

12. Multiplier Strip Gain Vs. Angle α of Strip

13. Electric Field Shape in Experimental Device

14. Silicon - Temperature - Resistance Characteristics

15. Multiplier Strip Gain Vs. Applied Voltage

16. Multiplier Strip Gain Vs. Applied Voltage

1. INTRODUCTION

The purpose of this contract was to develop and fabricate a small, purely electrostatic electron strip multiplier for use in small image dissector tubes designed for space navigation systems.

For the proposed application an electron multiplier one inch in length and with a gain of 10^6 was required.

The multiplication process can be described briefly as follows: The multiplier strip is mounted at an angle to the equipotential lines in a parallel field. (Figure 1). Primary electrons from a photoemissive cathode or a thermally excited source are directed at the negative end of the multiplier strip. The secondary electrons, released from the strip by the primaries, follow parabolic paths and land at a more positive point of the strip. The secondary emission cycle is then repeated.

Theoretical analysis of the secondary electron trajectories indicated that the angle of the strip with the normal to the field should be close to 20°. This was confirmed in the experiments.

The materials used for multiplier strips, besides having the necessary resistive and secondary emissive characteristics had to be stable in the presence of the alkali elements commonly used in photoemissive devices.

It was found in limited experiments that the resistance of gallium arsenide plates, cut from single crystals, was in the desired range but no multiplication could be obtained from either the plain or magnesium oxide coated plates. Thin films of tin oxide, nichrome, and silicon on lime soda glass slides with or without coatings of good secondary emitters, were evaluated. Of these, plain evaporated silicon with an overall resistance of 10^8 to 10^9 ohms proved to be the most successful. The high value

of resistance was necessary in order to minimize the power dissipation and the resultant joule heating of the strip. The maximum gain obtained from evaporated silicon strip was approximately 10^5.

2. THEORETICAL CALCULATIONS

The following discussion includes equations and calculations which were developed for the strip multiplier to determine the approximate strip slope and number of loops required to obtain a suitable overall gain with a selected voltage gradient. Figure 1 is a sketch, which briefly outlines the geometry of the strip multiplier.

In the development of the equations, certain assumptions were made to reduce the complexity of the theoretical treatment. It is first assumed that the initial velocity of electrons in the direction normal to the condenser plates is zero in calculations of average electron velocity. This assumption is reasonable, because the actual initial velocity is small compared with the final velocity resulting from the acceleration between plates. This means that only those secondary electrons leaving the strip in a direction parallel to the plates, i.e., at an angle (α) with respect to the strip, are considered in determining the loop length. Since α is a relatively large angle, the number of electrons emitted at/or close to α should be a high percentage of the maximum emission normal to the strip surface. Hence, the result should prove to be a close approximation of the average loop length.

Second, it is assumed that the initial velocity in the direction parallel to the plates is equal to one electron volt. Since the emission velocities essentially follow a maxwellian distribution, other velocities could be considered, but would provide no significantly better approximation for the average electron trajectory.

Although the above assumptions are made, it should be pointed out that variations in loop length will occur as a result of the various electron emission angles and velocities.

Let us consider trajectories of electrons accelerated normally between two parallel condenser plates in a uniform electrostatic field. The final energy of the electron is given by:

$$E = 1/2\ mv_f^2 = e\ V\ total$$

where

E = Final electron energy (ergs)

m = Electron mass = 9.1×10^{-28} grams

V_f = Final electron velocity (cm/sec.)

e = Electronic charge (coulombs)

V total = Voltage between plates (volts)

ρ = 1×10^7 ergs/joule

Hence, the final velocity is found to be

$$v_f = \left(\frac{2\rho e\ V\ total}{m}\right)^{1/2} \qquad \text{where } \frac{e}{m} = 1.759 \times 10^8 \ \frac{\text{coulombs}}{\text{gram}}$$

Since it is assumed that the initial velocity normal to the plates is zero, the average velocity of these electrons is given by

$$v_{av} = \frac{v_f}{2} = 1/2 \left(\frac{2\rho e\ V\ total}{m}\right)^{1/2}$$

The average velocity can also be expressed as $v_{va} = \frac{S}{t}$ where S is the distance travelled.

Hence, the time of flight of the electron between the plates can be written as

$$t = \frac{S}{v_{av}} = \frac{2S}{v_f} = 2S \left(\frac{2\rho e\ V\ total}{m}\right)^{-1/2}$$

Now let us consider electrons emitted in a direction parallel to the plates. Since there is no field component in this direction, no acceleration takes place and the average velocity is equal to the initial velocity. This direction will be referred to as the "r" direction. The distance traversed by an electron in the "r" direction is given by:

$$r = v_r t$$

where v_r is the electron velocity in the "r" direction and t is the time of flight discussed above. This velocity can be expressed as

$$v_r = \left(\frac{2E_r}{m}\right)^{1/2}$$

where E_r is the energy of the electrons emitted in the "r" direction.

Figure 1 shows that the loop length or the distance between loop nodes along the strip is defined by the vector sum of the "r" and "s" distances travelled during the time of flight (t). The loop length is given by:

$$B = \frac{S}{\sin \alpha}$$

where $\alpha = \tan^{-1} \frac{S}{r}$

and $$S = \frac{L}{N}$$

where L is the perpendicular distance between plates and N is the effective number of multiplier stages.

The effective stage voltage can be written as:

$$V = \frac{V \text{ total}}{N} = \frac{S}{L} \quad V \text{ total}$$

Since the overall gain (G) can be written as a function of the stage gain, i.e.,

$$G = \gamma^N$$

the stage gain required to obtain an overall gain G can be determined from the equation

$$\gamma = \text{anti log} \left[\frac{\log_{10} G}{N}\right]$$

With the equations given in the preceding paragraphs, loop length and strip angle approximations can be calculated as follows:

Assuming that L, the distance between plates = 2.5 cm,

G, the overall gain = 1×10^6

V, the overall voltage = 1600 volts

Vs, the stage voltage = 32 volts

(E_r), the energy of electrons emitted in the "r" direction = 1 electron volt = 1.6×10^{-12} ergs

The number of stages (N) is then given by

$$N = \frac{V}{Vs} = \frac{1600}{32} = 50 \text{ stages}$$

The secondary emission ratio required to obtain a gain of 1×10^6 with 50 stages of amplification is calculated as

$$\gamma = \text{anti log} \left(\frac{\log_{10} G}{N}\right) = \text{anti log} \left(\frac{\log 1 \times 10^6}{N}\right)$$

$$\gamma \sim 1.13$$

This secondary emission yield should be obtainable from both cesium antimony and magnesium oxide secondary emission surfaces at the stage voltage indicated.

Since we have set the number of stages at 50 and the total distance between plates at 2.5 cm the distance (S) indicated in Figure 1 can be caluclated by

$$S = \frac{L}{N} = \frac{2.5}{50} = 5 \times 10^{-2} \text{ cm}$$

where S is the component of the electron trajectory normal to the condensor plates, associated with one stage of amplification or one loop.

Knowing S and V_s the time of flight for the electron to form one loop can be obtained by

$$t = 2S \left(\frac{2\rho eV_s}{m}\right)^{-1/2} = 2 \times 5 \times 10^{-2} \left(2 \times 1.759 \times 32 \times 10^{8} \times 10^{7}\right)^{-1/2}$$

$$t \sim 3 \times 10^{-10} \text{ sec.}$$

Using the equation

$$v_r = \left(\frac{2Er}{m}\right)^{1/2}$$

and setting $Er = 1.6 \times 10^{-12}$ ergs,

the velocity of the electrons in a direction parallel to the condensor plates can be calculated as follows:

$$v_r = \left(\frac{2 \times 1.6 \times 10^{-12}}{9.1 \times 10^{-28}}\right) \sim 5.92 \times 10^{7} \text{ cm/sec}$$

and the distance (r) can be obtained by

$$r = v_r t = 5.92 \times 10^{7} \times 3 \times 10^{-10} \sim 1.78 \times 10^{-2} \text{ sm}$$

The strip slope can now be determined by the equation

$$\tan \alpha = \frac{S}{r} = \frac{5 \times 10^{-2}}{1.78 \times 10^{-2}} \quad 2.82$$

$$\alpha = 70.5°$$

and the loop length (B) is calculated as

$$B = \frac{S}{\sin\alpha} = \frac{5 \times 10^{-2}}{.943}$$

$$B \approx 5.3 \times 10^{-2} \text{ cm}$$

The total strip length (b) is given by

$$b = \frac{L}{\sin\alpha} = \frac{2.5}{.943} = 2.65 \text{ cm}$$

The values obtained above should be close approximations to the actual strip performance, but it should be pointed out that the peak characteristics can only be determined experimentally.

Although the required gain of 10^6 was not achieved, the experiments, conducted in this investigation demonstrated the feasibility of using the strip multiplier in photoemissive tubes.

Materials limitations and the necessity of using high accelerating voltages much in excess of 1600V prevented the realization of the required gain.

3. RESISTIVE STRIP DEVELOPMENT

One object of this contract was to develop resistive electron multiplier strips, exhibiting secondary emission properties and stable resistance in the range of 10^8 ohms.

In the process of resistive strip development several approaches, employing various resistive and secondary emissive materials, were considered.

During the initial experiments, the possibility of using magnesium oxide, a good secondary emitter, for the strip multiplier surface, was investigated.

Films of magnesium oxide and silver doped magnesium oxide on soda lime glass were made and their resistive properties evaluated. The resistance of these films proved to be too high for the proposed application. Soda lime glass was selected for the experiments since it was necessary to avoid the use of glasses containing lead as these react with the alkali elements which would be used in devices utilizing the multiplier. Vacuum deposited nichrome was tried next for resistive strip application. Continuous nichrome films with an optical transmission of 80% had a resistance of only 3×10^5 ohms. Since such a thin layer could not carry the high conduction current without overheating and ultimate breakdown a "ladder" configuration of nicrhome film was adapted as shown in Figure 2. This type of resistive film strip with cesium antimony secondary emissive layer was used in first four experimental devices.

The initial resistance of the first batch of "ladder" type nichrome films of about 8×10^6 ohms was too low for use in the strip multiplier devices

although one of them was used in the first experimental tube.

Further work on "ladder" type nichrome films resulted in resistive strips with maximum resistance, varying between 50 and 90 megohms. However, these films were unable to withstand voltages necessary to attain the required gain.

In search for other applicable resistive strip materials experiments were conducted to evaluate nesa and silicon films. Nesa films of the required resistance (10^8 ohms) did not appear to form a continuous layer and in addition the voltage current relationship of the films was non linear. In view of these undesirable characteristics and the instability of nesa in the presence of the alkali elements this approach was abandoned.

Vacuum deposition of pure silicon on glass slides yielded films which exhibited stable resistance at voltages up to 4 kilovolts both in vacuum and in air. With these, practically any desired value of resistance was obtained in the range from 10^3 to 10^9 ohms, by careful control of deposition rate, temperature of the substrate and pressure. Of all the materials investigated, evaporated silicon films proved to be most suitable for multiplier strip application.

The possibility of using strips of solid silicon and gallium arsenide was considered. Although some of the samples exhibited suitable resistance characteristics, the secondary emission, from both uncoated and magnesium oxide coated strips, was very low.

4. EXPERIMENTAL TUBE DEVELOPMENT

Initially it was intended that an electrostatically focussed electron gun would be used as the source of primary electrons in strip multiplier experiments. However, the difficulties encountered in controlling the extremely small currents prompted the development of experimental tubes using photoemissive cathodes for the electron source. In these, it was possible to produce a low density small cross section beam of electrons with which to evaluate the electron multiplier design and strip characteristics.

This approach also ensured that the strips were exposed to similar environmental conditions to those which would occur in their ultimate use.

The experimental device was designed around the image section of the CBS Type CL 1147 Image Dissector. No deflection system was included since the position of the electronic spot at the negative end of the multiplier strip, which was placed directly below the aperture, could be controlled by physical displacement of an optical image at the photocathode. The area on which primary electrons could land on the multiplier was determined by an aperture 0.030 by 0.140", the major axis of which was parallel to the plane of the multiplier strip. Figure 3 is a schematic of the design.

Some of the devices were made so that the angle which the strip made with the electric field could be varied. This enabled rapid confirmation of the angle at which maximum gain occurred.

The initial design proved unsatisfactory owing to leakage between the field shaping electrodes being in the same order as the strip multiplier

currents. In addition test measurements indicated that electrons from the strip were being collected by the field shaping electrodes. Redesign of the collector support eliminated these problems.

During the tube experiments several changes were made in the field shaping electrode configuration in order to study their effect or gain since the optimum theoretical approach had to be compromised in the mechanical design. The changes included using a multiplicity of shaping electrodes, using the high potential field shaping electrode as the collector and changes in the relative position of the multiplier strip within the electric field.

5. EXPERIMENTAL TUBE: TEST AND DISCUSSION

The design objective was to obtain a minimum gain of 10^6 at maximum potential of 1600 volts applied to the multiplier strip.

All the experimental strip multiplier tubes were tested with the image section energized as shown in Figure 3. The collector potential was set about 100 volts positive with respect to the bottom end of the strip.

The measured gain of the first strip multiplier tube, Serial No. 607A was low due to leakage paths between the tube elements. In addition low nichrome film resistance (8×10^6 ohms) prevented the application of high voltages which were necessary in order to obtain practical gains.

Figure 4 shows the strip conduction current versus strip voltage curve.

Figure 5 shows the curves of gain versus strip voltage for this tube.

The gain curves of Figure 6 were obtained when retesting the same tube after cleaning up of leakage paths. The strip resistance measured during the retesting varied from 50 to 200 megohms depending on the applied voltage. The maximum gain upon retest was 136,000. This was measured when the strip was at 4° with respect to the tubes axis when the grid potential was near that of the negative end of the strip.

In tube Serial No. 610F a nichrome film resistive strip of 80×10^6 ohms was used. The angle, that the strip was making with the axis of the tube or normal to the condenser plates, was fixed at 19.5°. The test data of this tube indicated that the grid potential had a significant effect on the overall performance of the strip multiplier. Figure 7 shows a curve of gain versus multiplier strip voltage obtained by adjusting the

grid voltage at each strip potential for maximum gain. Figures 6 and 7 show that the maximum gain of tube number 610F was almost identical to that of tube 607A; when the angle the latters multiplier strip made with the tube axis was 20°. The maximum gain of both devices occurred at the same overall voltage, approximately 1400 volts. No further increase of gain was obtained by increasing the strip voltage and in fact, increasing the voltage caused a decrease in gain. The precise reason for this fall was not determined. Distortion of the electric field which was maintained by relatively remote electrodes or temporary loss of minute quantities of cesium due to joule heating of the strip are feasible causes.

Figure 8 is a schematic diagram of tube Serial No. 620F. The major design feature of this tube was the multiple grid structure surrounding the strip. The test results of this tube, again show the dependence of gain on electric field shaping by the grids. The low gain of this tube was attributed to the poor secondary emissive characteristics of the particular strip. Further consideration of this, subsequent field plots and bell jar experiments indicated, that with the strip mounted at 19.5° with respect to the equipotential lines, the desired field configuration would be achieved.

The measured grid currents did not show a definite increase with the decrease of gain which indicates that there was no excessive collection of secondary electrons by the grid and that the shape and strength of the electric field were the major factors determining the gain of the tube. The resulting gain curves are shown in Figure 9 .

One tube was made employing a silicon resistive strip. This tube was not tested due to the 80% decrease in multiplier strip resistance caused by tube processing. Other silicon resistive films, exposed to standard tube processing in glass enclosures, exhibited stable characteristics at up to 3.5 kilovolts.

The overall test data of strip multiplier tubes clearly indicated the need for detailed investigation of the electric field configuration and its effect on the performance of the multiplier strip.

The tests also showed the necessity for further evaluation of resistive strip materials.

6. PARALLEL FIELD EXPERIMENTS

To confirm the test results of strip multiplier tubes an experiment was designed to evaluate the performance of the multiplier strip in a practically distortion-free parallel electric field. Figure 10 shows a schematic of the electron gun and the multiplier strip assembly used in the experiment.

The information obtained from this experiment consisted of:

1. Multiplier strip gain characteristics, as a function of voltage, and angle of inclination,

2. electrical and physical properties of strip materials,

3. the potentials necessary for attaining practical gains from the multiplier strip,

4. the effect of electric fields on the gain of strip electron multipliers; and

5. confirmation of suspected electron loss to the field shaping electrodes.

The greatest gain was obtained with a 700 megohm silicon film on a glass substrate. Gain vs. applied voltage curves are shown in Figures 11 and 12. Figure 11 shows gain vs. strip multiplier voltage at five different angles α of strip inclination with the vertical axis. A gain of 148,000 was obtained when the angle of the strip made with the vertical axis was $20° \pm 1°$. This gain was obtained with the strip potential of 3750 volts, which was the maximum potential used in this experiment.

The curves indicate that much higher voltages were needed to get the required gain. Since the resistance temperature coefficient of silicon,

as shown in Figure 14, is negative the power dissipation of the strip had to be kept below 50 milliwatts in order to prevent progressive decrease in strip resistance and ultimate breakdown. Figure 14 shows the published [1, 2, 3] resistance temperature curves for bulk silicon and also those for evaporated silicon films made under this program.

Silicon film strips with resistance of 750 megohms were successfully made. These strips were operated satisfactorily, at room temperature, with an overall potential of 4000 volts.

As shown by the curves of gain versus angle (Figure 12) the gain of the multiplier strip increased as the angle was approaching 20°. As soon as the angle became larger than 20°, a sharp drop in gain occurred.

As stated in section 3 of this report, the maximum gain of Tube No. 1 was obtained with the strip angle at 4° with respect to tube axis. However, this occurred when the grid electrode potential was close to that of the negative end of the strip. Even when the grid was disconnected, this was so, because of the high conductive path between negative end of the strip and the grids. Therefore, in each case the field shape would have been similar to that sketched in Figure 13, which shows that the angle of the strip made with the normal to the field was approximately 20°.

The angle for maximum secondary yield in a practically perfect parallel electric field for a constant energy of primary electrons appears to be about 20°.

This agrees substantially with the assumptions made in the theoretical calculations.

No significant gains were obtained from magnesium oxide coated silicon and gallium arsenide resistive strips; however, Figures 15 and 16 do show

that the 20° angle of the multiplier strips yielded highest gains.

The low gain of both strips might be attributed to low secondary yield of magnesium oxide due to possible contamination of the oxide layer.

No gain was obtained with a plain gallium arsenide resistive strip.

In order to substantiate the suspected loss of electrons from the edge of the strip to the grids, gains of one inch and 1/2 inch portions of the same multiplier strip were measured. If there was no loss of electrons to the field shaping grids with the voltage gradient the same in each case, the gain of the one inch long strip would have been equal to the square of the gain of the one-half inch long strip. However, the gain of the longer strip was only double (1730 compared with 860) that of the shorter strip.

Additional confirmation, that secondary electrons were being collected by the field shaping electrodes, was obtained by operating the 1" long and the 1/2 inch long strips at the same overall voltage. Under these conditions the gain of the shorter strip was greater than that of the longer. (800 compared with 456). If there was no loss of electrons to the field shaping grids the gain would have been the same in each case.

The loss of secondary electrons to the grids can be attributed to their initial energy distribution and their direction of emission from the multiplier surface. These factors result in the spreading of the cascading "beam" of electrons as it progresses along the multiplier strip. When the spreading electron "beam" becomes as wide as the strip itself a certain proportion of the electrons emitted from points near the edge follow trajectories which

terminate on the surfaces of the field shaping electrodes. To some extent this loss can be eliminated by using a "bell" shaped field; however, if the multiplier strip has to be long in order to get the required gain, the multiplicity of electrodes necessary to provide the "bell" shaped field would eliminate the advantages of the strip multipliers simplicity.

A second solution would be to widen the multiplier strip and provide the multiplicity of electrodes, with which to maintain a parallel electric field within an operational device. Again, the complexity and size of a strip multiplier made to give the required gain would be greater than that of conventional multiplication devices.

The peak gain of the strip in the "bell" shaped field was higher than that obtained with 1/2 and one inch strips, at the same voltage, in the parallel field indicating smaller loss of electrons to the grid in the "bell" shaped field.

7. CONCLUSIONS

The feasibility of making a strip electron multiplier was demonstrated. However, it is evident that serious limitations do exist which prevent the manufacture of a small, high gain strip multiplier which can handle relatively high input currents. For example, the light flux from the Star Canopus, focussed into a 10^{-8} lumen spot, impinging on a 40 microampere per lumen photocathode would produce an input current of 4×10^{-13} amperes and if the strip gain is 10^{6}, an output current of 4×10^{-7} amperes.

A small device with a simple electrode configuration was made. The maximum gain of this, with the electrode potentials adjusted to give a "bell" shaped field was in the order of 10^{5}. The feasibility of the approach was demonstrated further during the parallel field experiments, however, it was found that material limitations do not allow the construction of a small device which will have sufficient gain and current output capability. The same limitations will apply equally to single channel and multichannel tubular electron multipliers based on similar theoretical approaches.

It is concluded that a strip multiplier could be made to perform the functions of the conventional, focussed type electron multiplier, now being used in the Canopus star tracking system image dissectors. However, a practical device which would fulfill these functions would in all probability be larger and more complex than the conventional multipliers presently used. For these reasons it is recommended that further effort be directed towards the design and development of miniaturized electron multipliers using conventional secondary emissive surfaces and electrodes.

8. REFERENCES

1. J. Millman, "Vacuum Tube and Semiconductor Electronics". Pg. 82, Eg. 3-30 and Table 3-1

2. G. L. Pearson and W. H. Brattain, "History of Semiconductor Research", Proc. IRE, 43, 1794 - 1806, Dec., 1955

3. E. M. Conwell, "Properties of Silicon and Germanium", Proc. IRE, AO 1327 - 1337, Nov. 1952

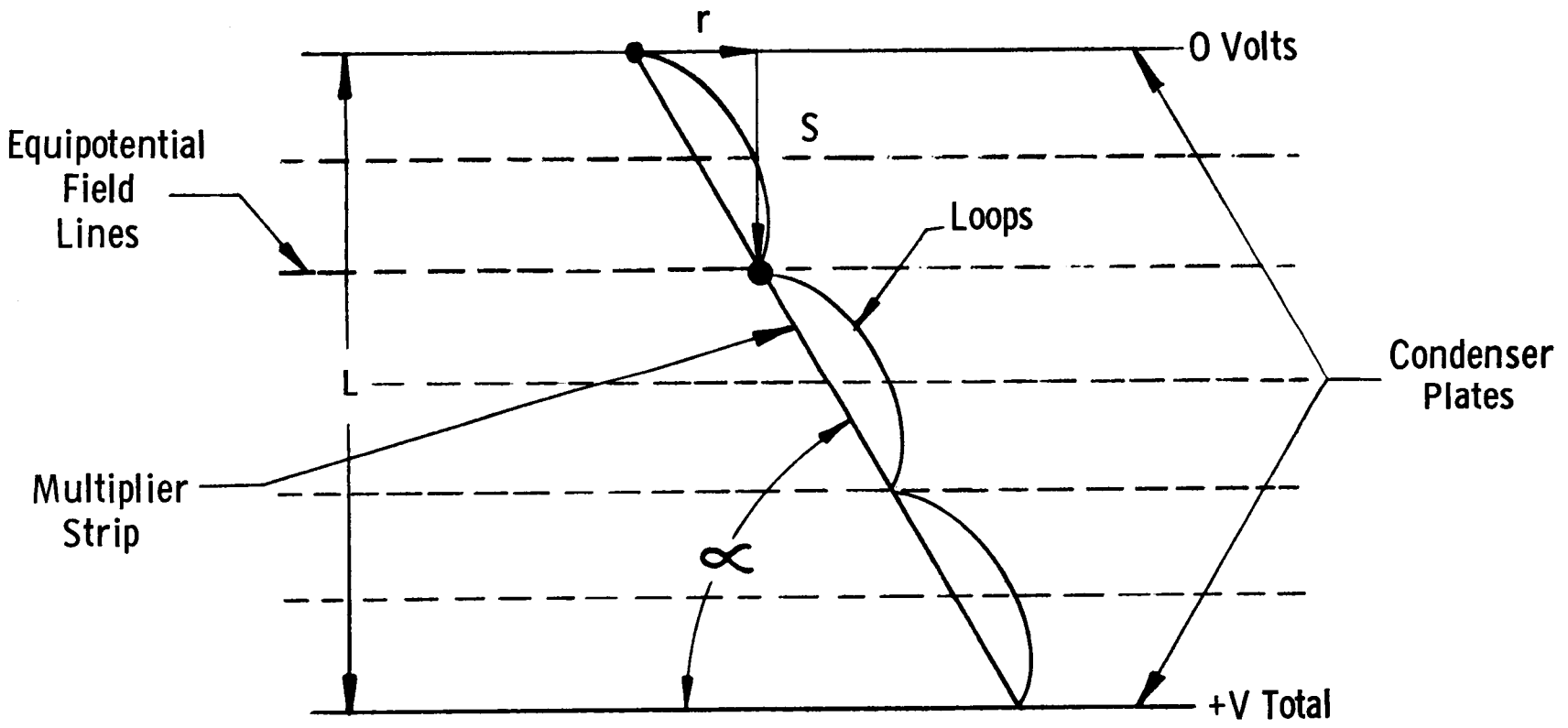

Multiplier Strip in Parallel Electric Field.

Figure 1

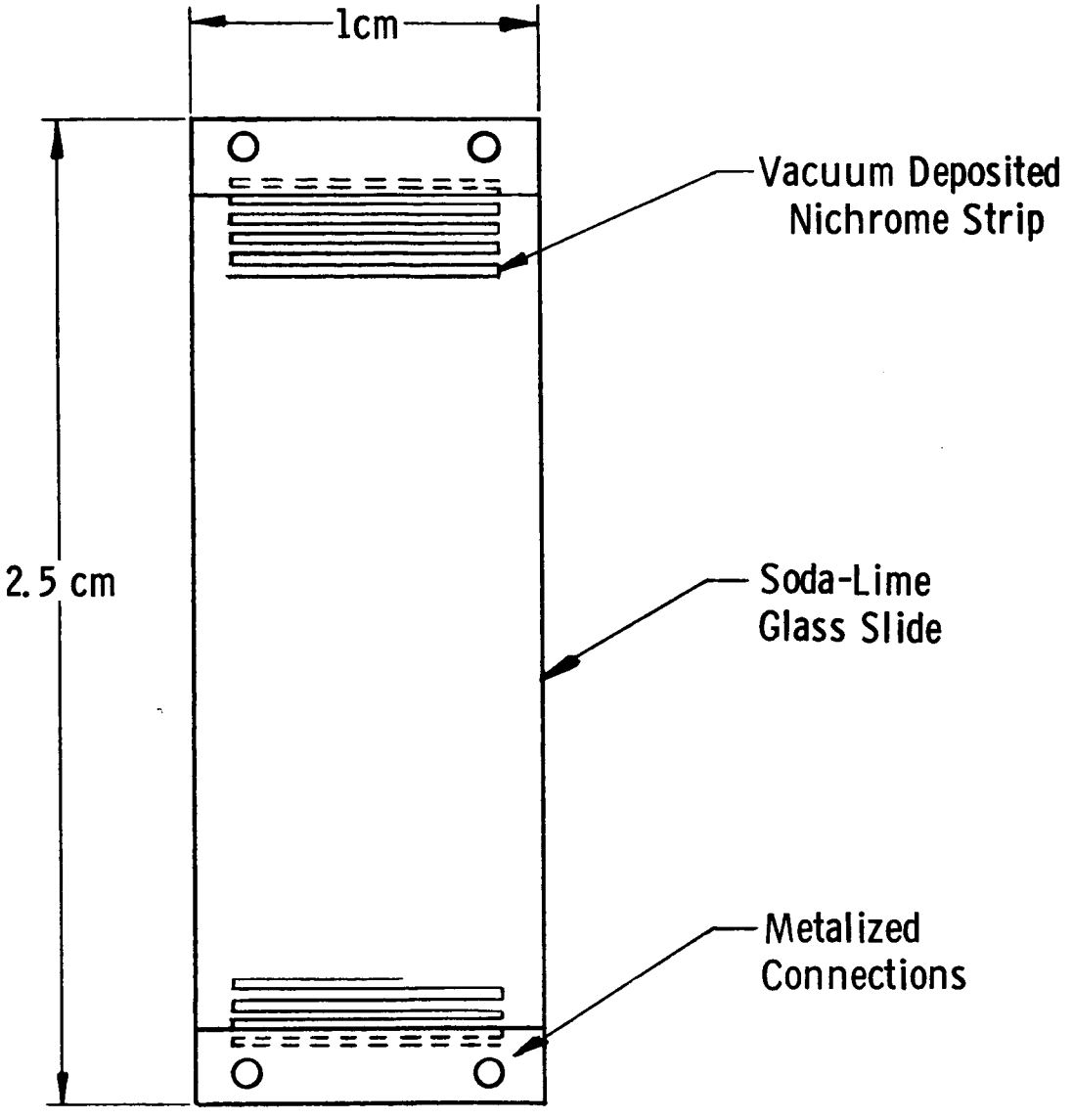

Design of Ladder Type Nichrome Film
Multiplier Strip

Figure 2

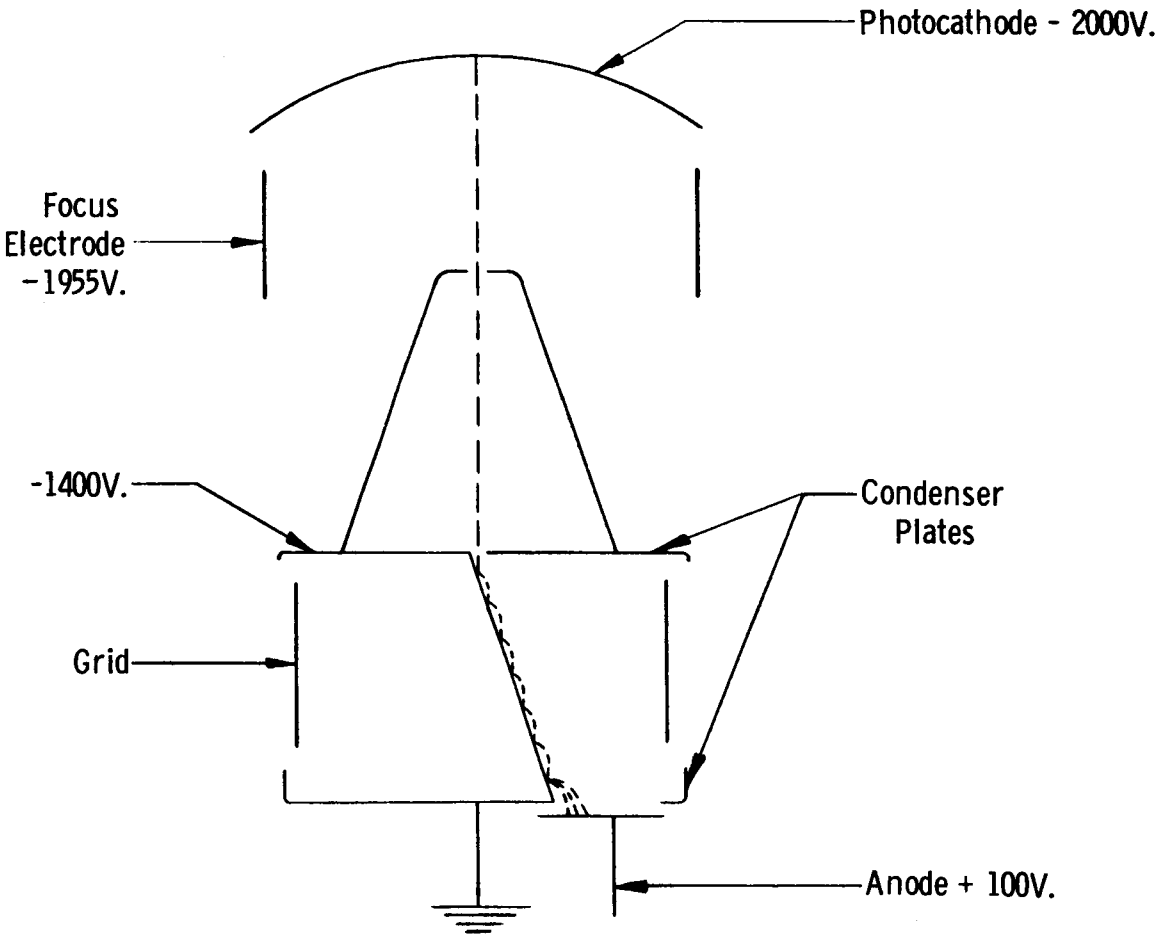

Schematic of Experimental
Strip Multiplier Tube

Figure 3

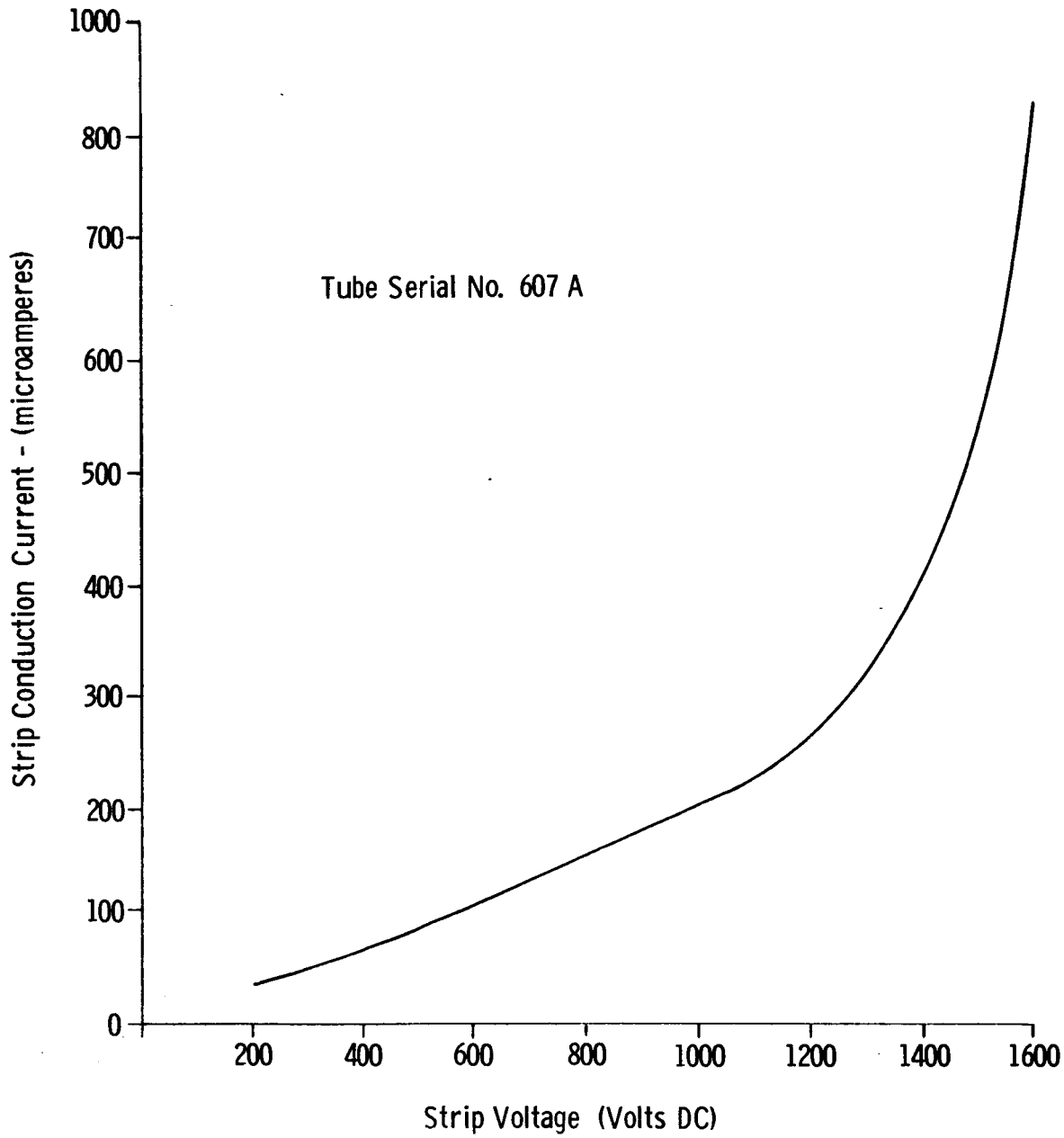

Effective Strip Conduction Current vs. Applied Voltage
(First Experimental Strip Multiplier)

Figure 4

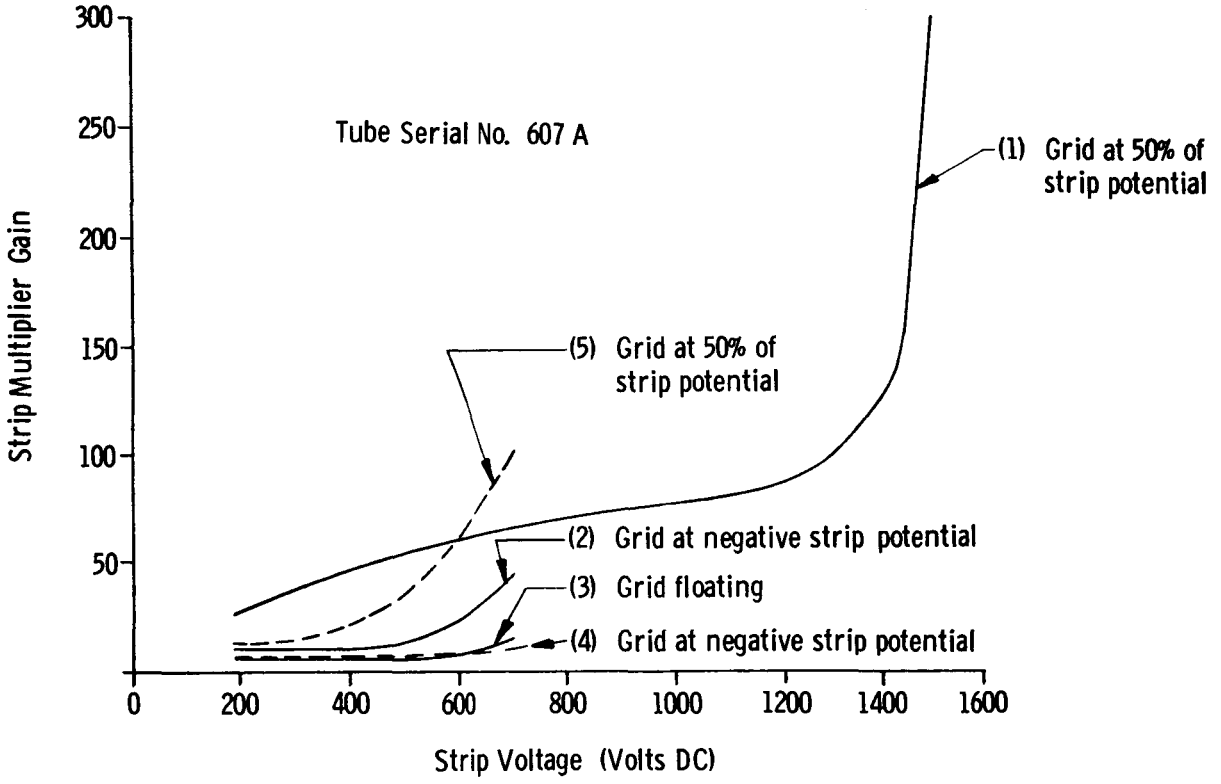

Test Conditions

1. General
   Image section voltage = 500 Volts
   Focus electrode voltage = 50 Volts with respect to photocathode
   Collector voltage = 90 Volts with respect to the bottom of the strip

2. Curves 1, 2, and 3
   Strip resistance = 7×10^6 ohms
   Leakage resistance (Bottom of strip to grid) = 6×10^6 ohms
   Leakage resistance (Top of strip to grid) = 2×10^5 ohms
   Strip angle = 15° with the vertical

3. Curves 4 and 5
   Strip resistance = 8×10^6 ohms
   Leakage resistance (Bottom of strip to grid) = 6×10^6 ohms
   Leakage resistance (Top of strip to grid) = 1×10^6 ohms
   Strip angle = 25° with the vertical

Strip Multiplier Gain vs. Applied Voltage
(First Experimental Strip Multiplier)

Figure 5

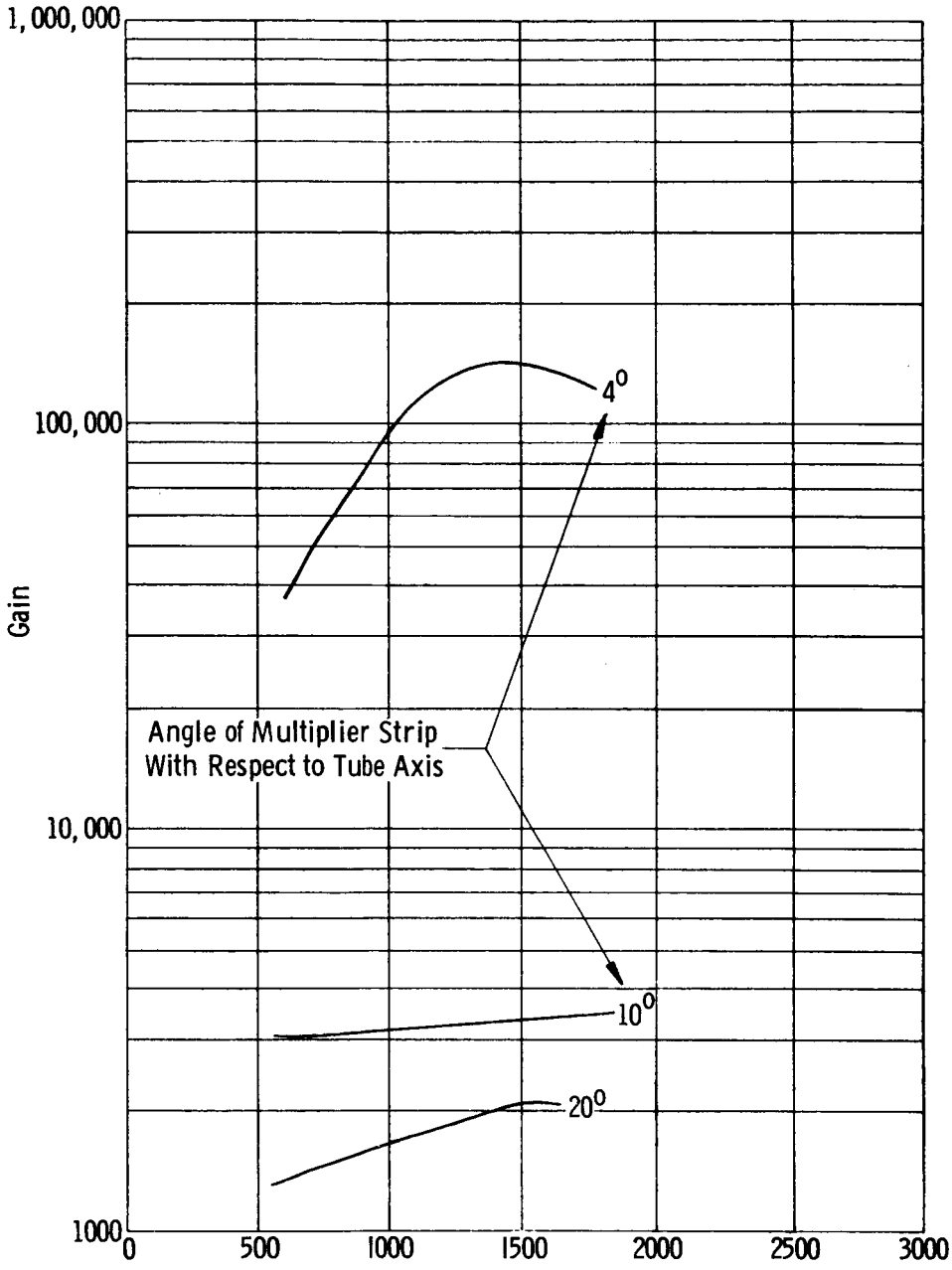

Multiplier Gain vs. Applied Voltage
(First Experimental Strip Multiplier)

Tube Serial No. 607 A

Figure 6

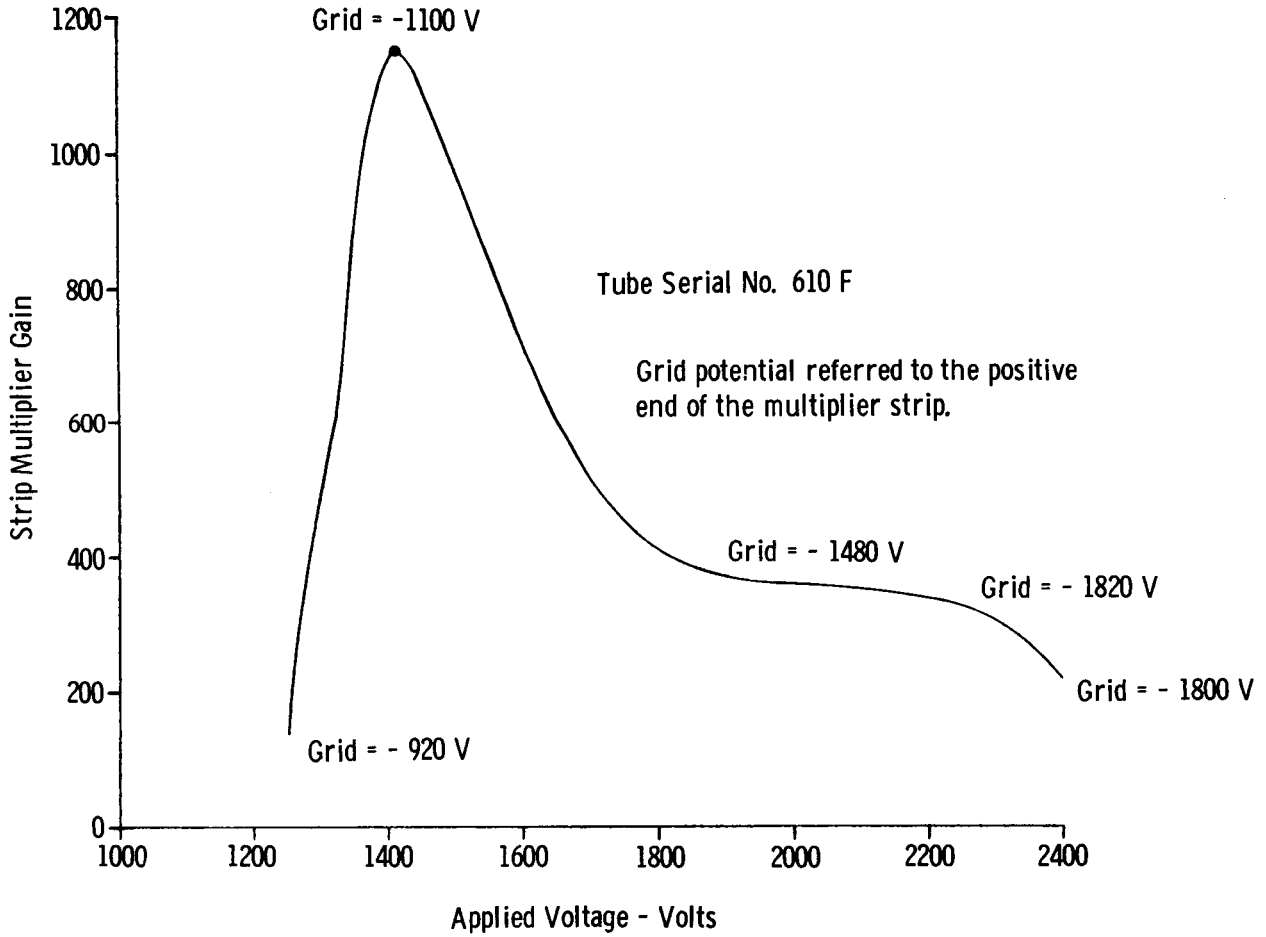

Strip Mutliplier Gain vs. Applied Voltage
Grid Potential Adjusted For Maximum Gain
(Second Experimental Strip Multiplier)

Figure 7

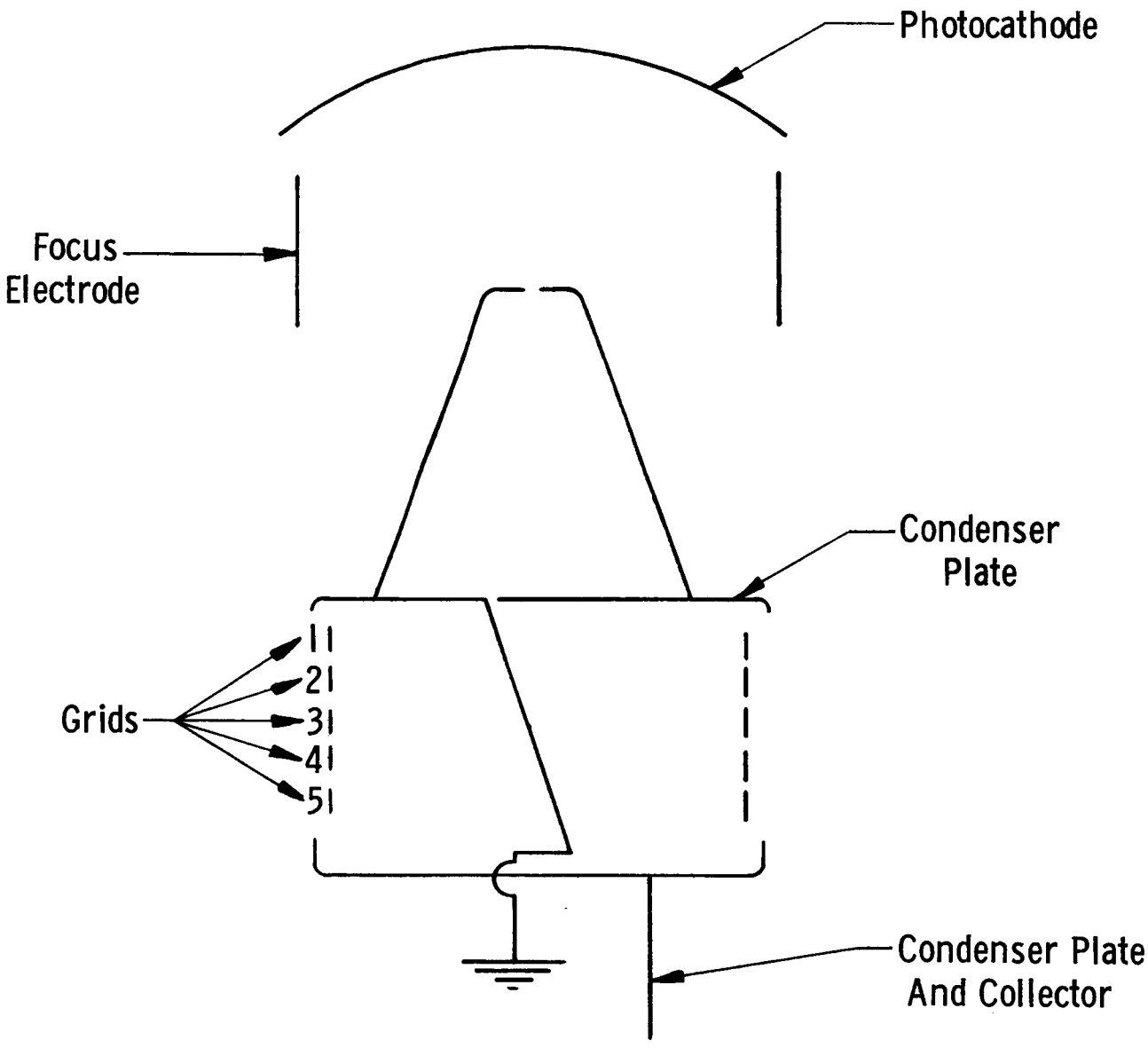

Schematic of Experimental
Strip Multiplier Tube

Figure 8

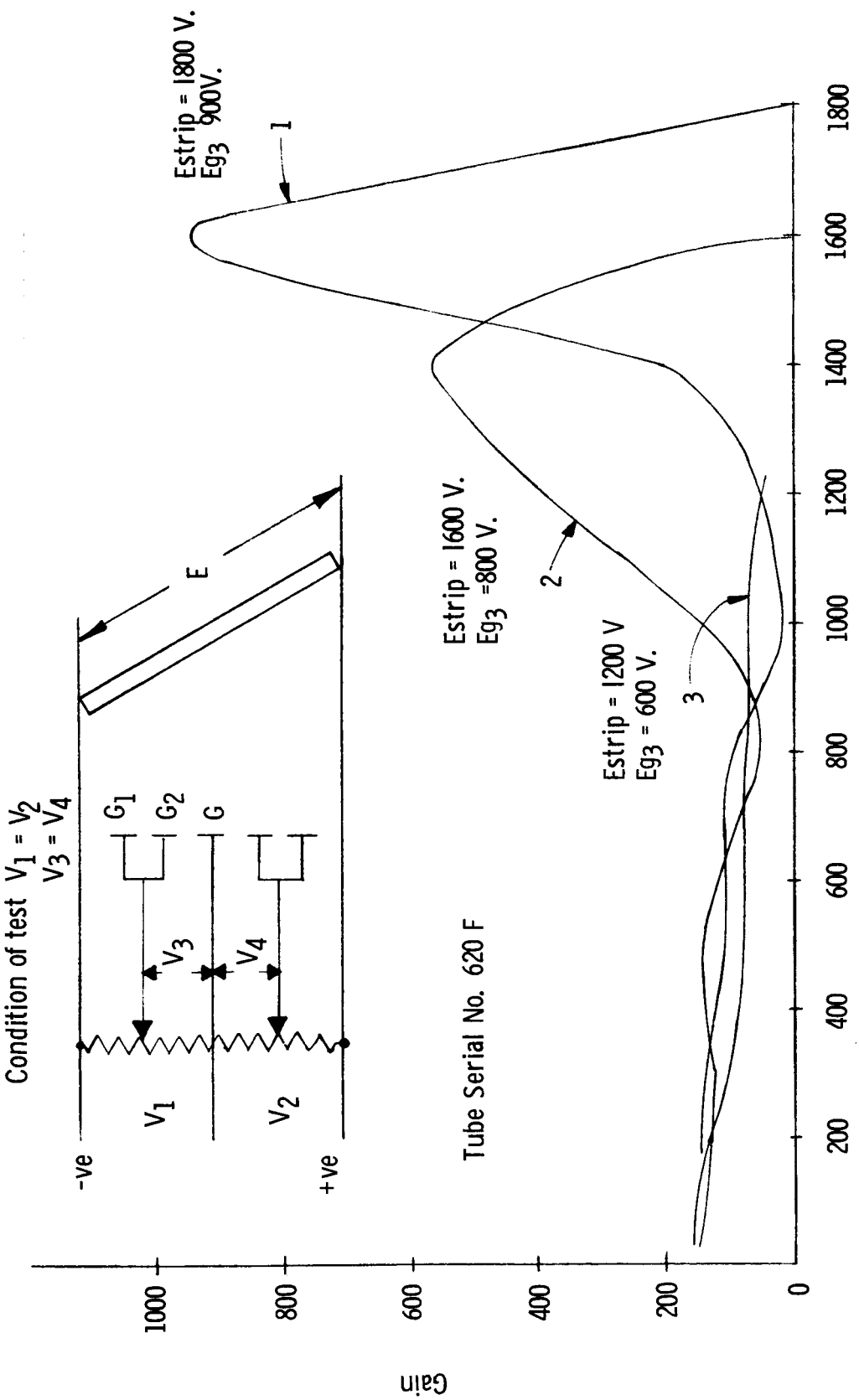

Electron Multiplier Gain
(Multiple Grid Design)

Figure 9

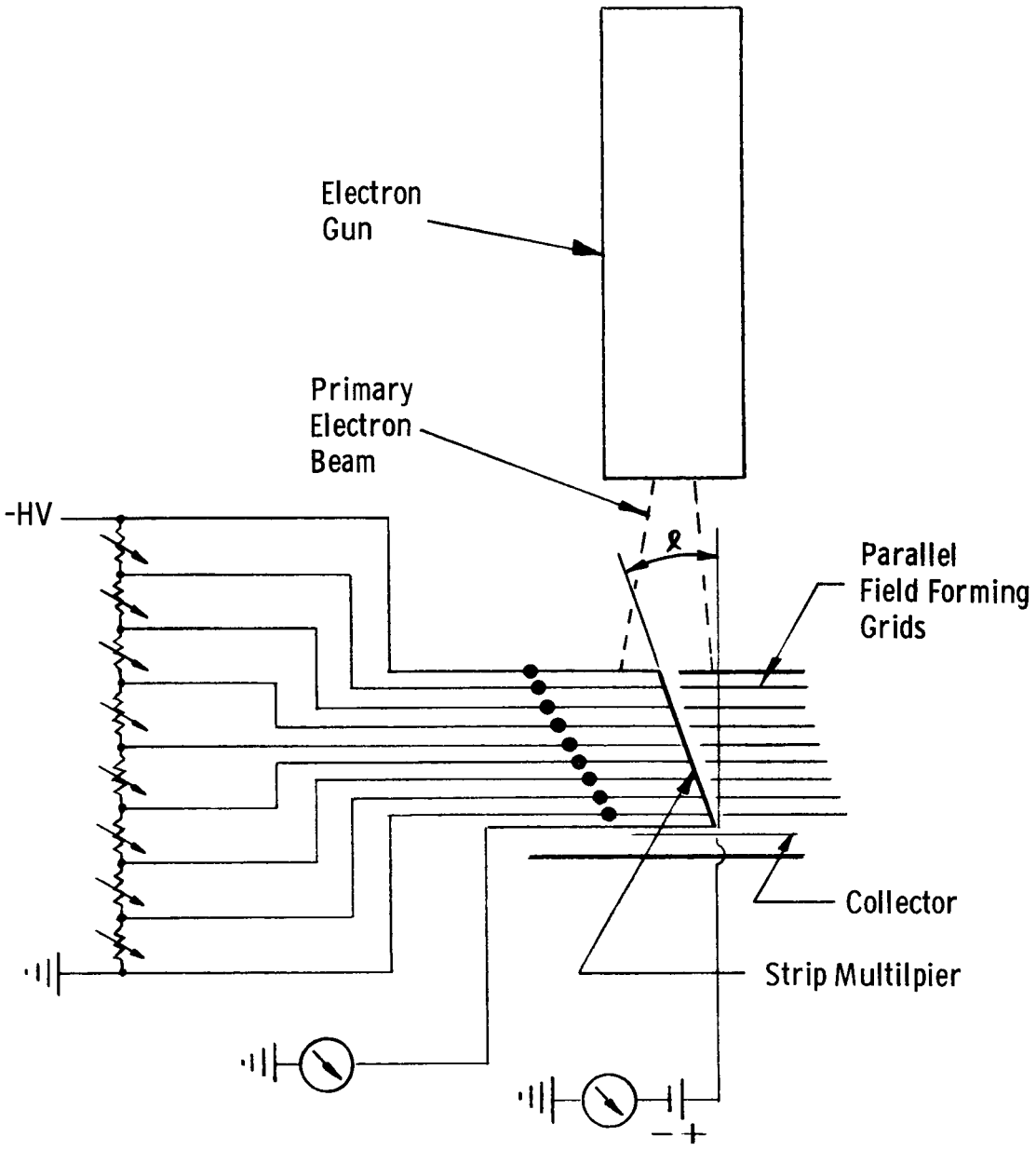

Shematic Of Parallel Electronic Field Experiment

Figure 10

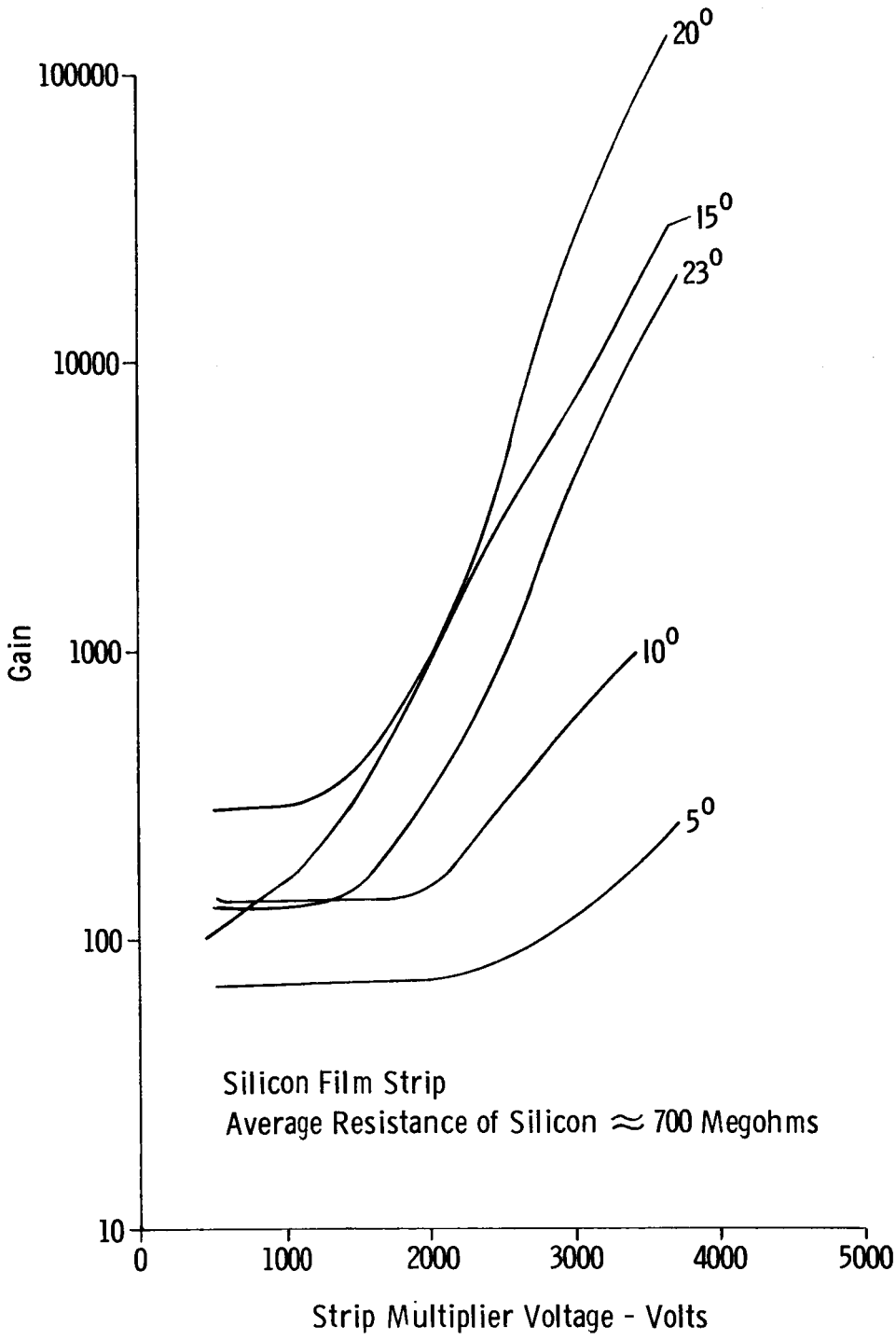

Multiplier Strip Gain Vs. Applied Voltage

Figure 11

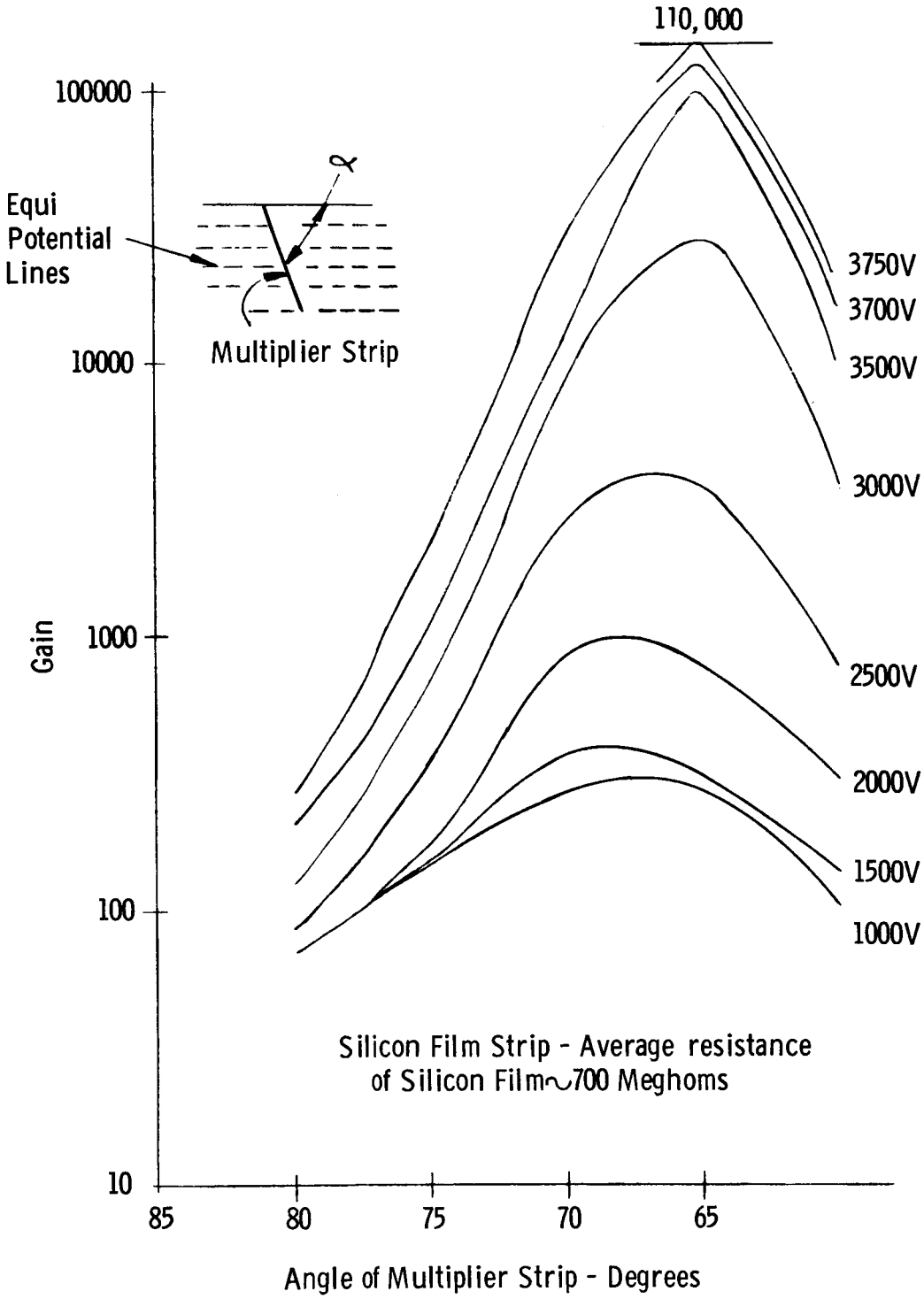

Multiplier Strip Gain vs. Angle of Strip

Figure 12

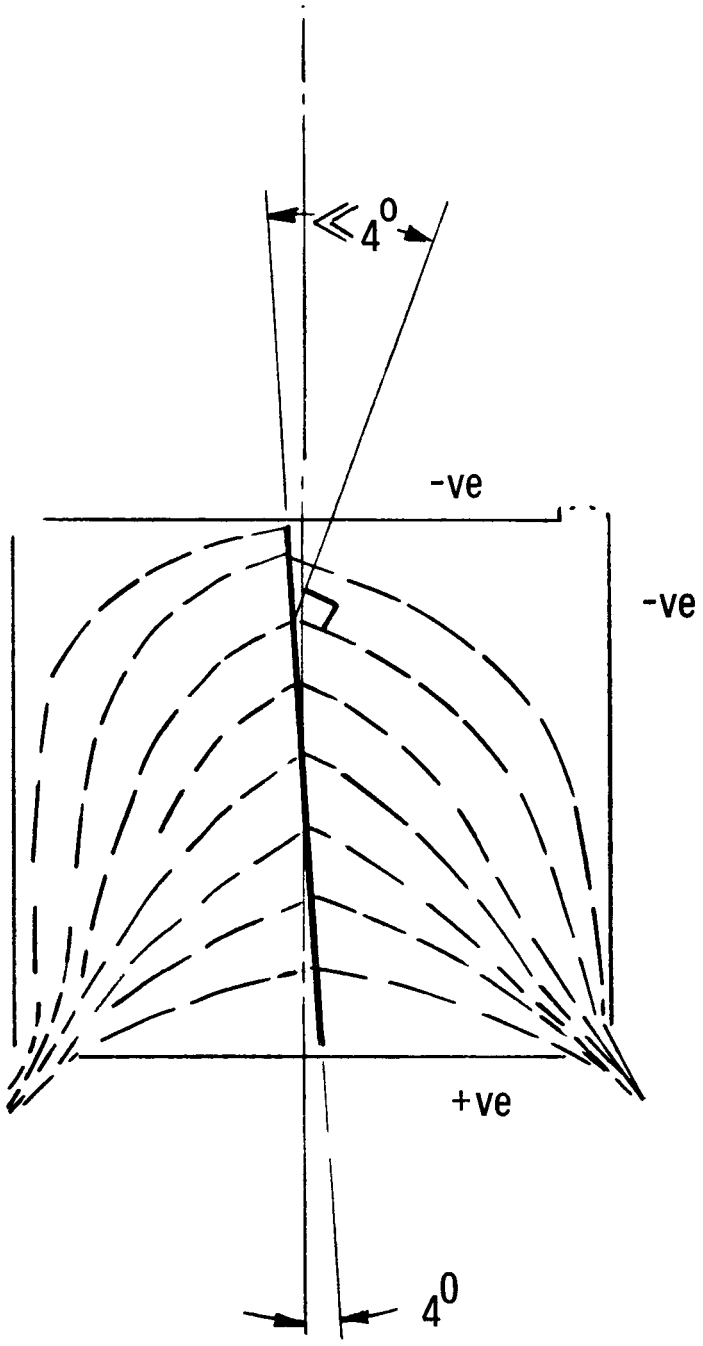

Electric Field Shape in Experimental Device

Figure 13

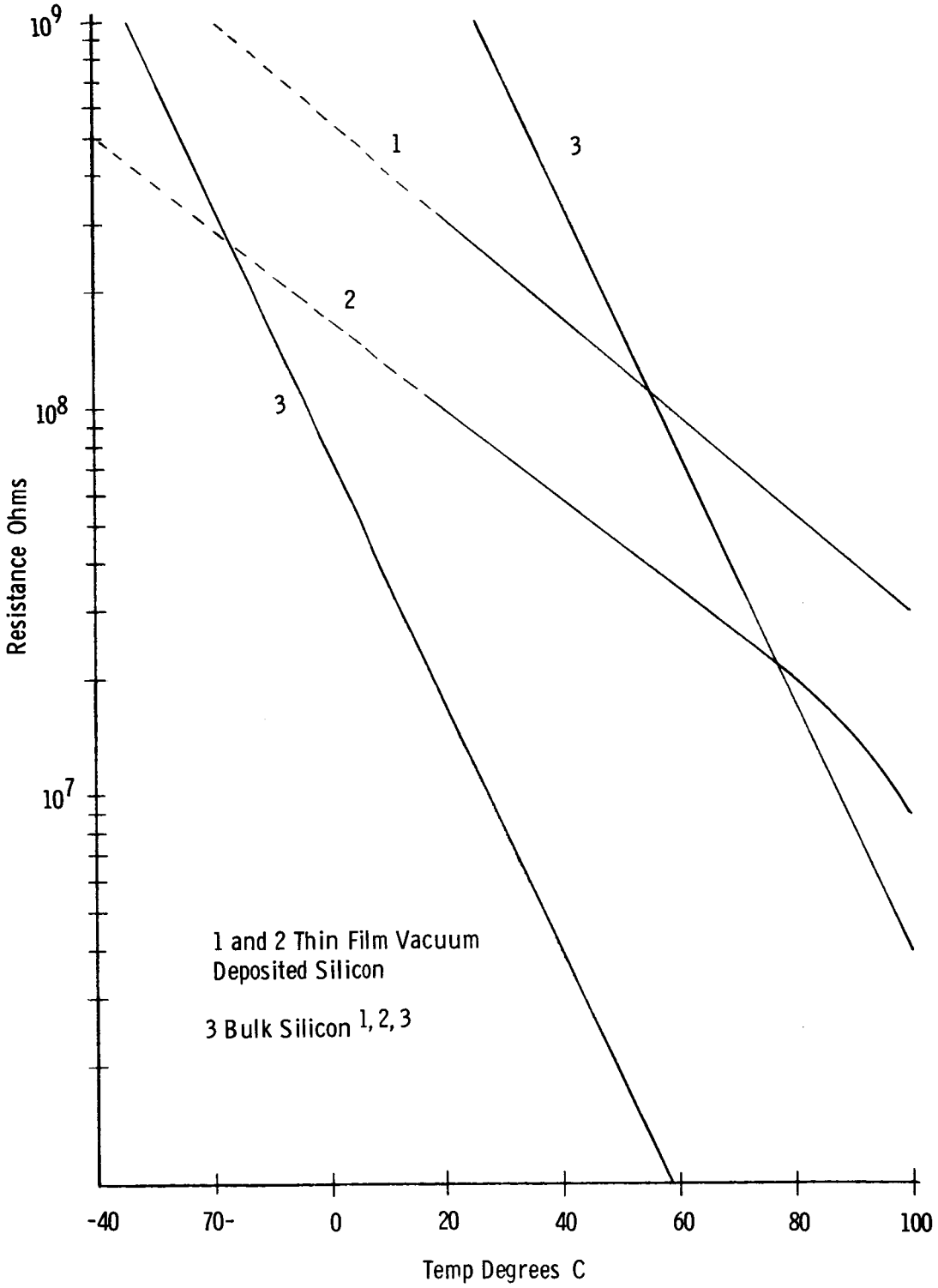

Silicon
Temperature/Resistance Characteristics

Figure 14

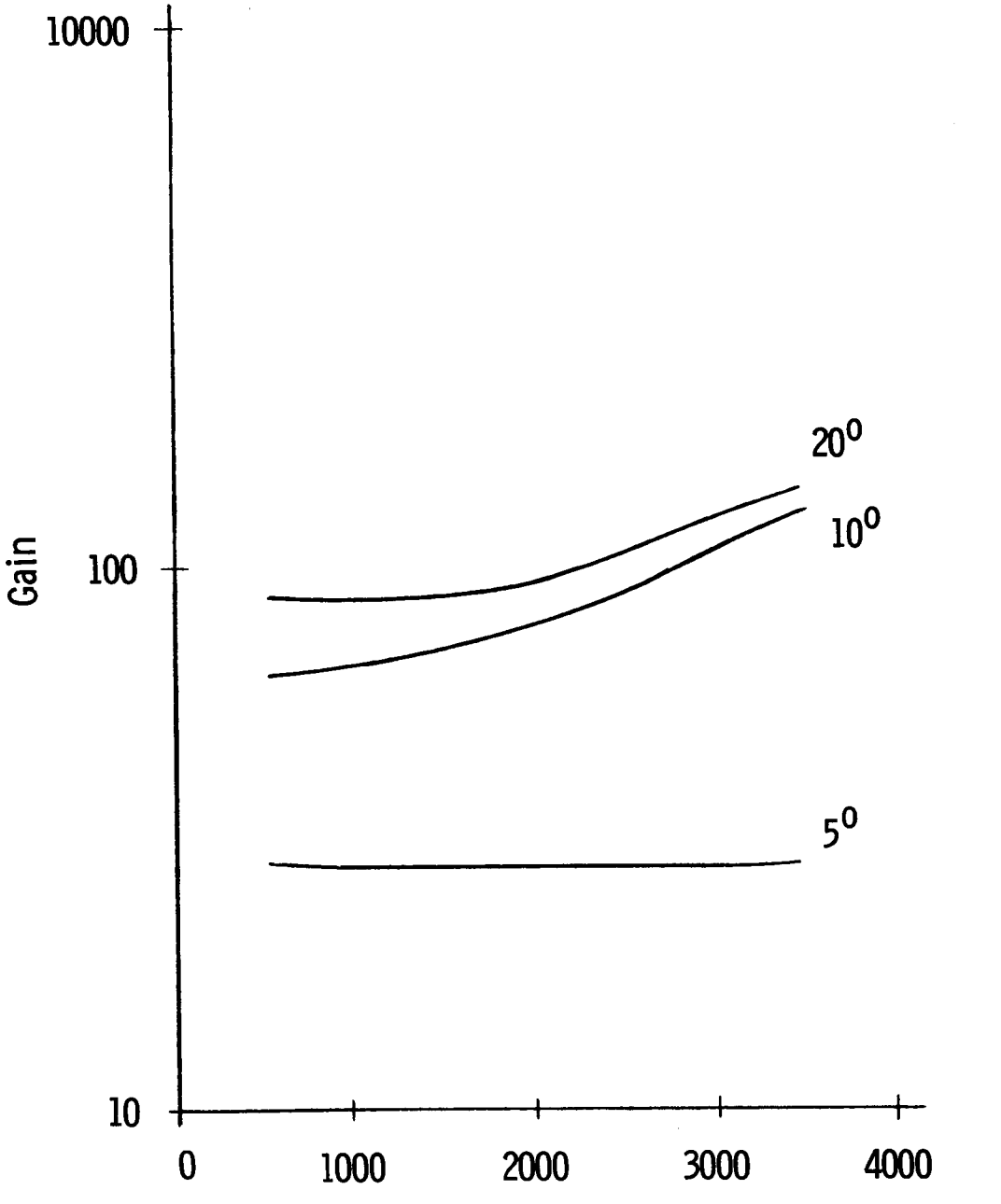

Multiplier Strip Gain vs. Applied Voltage

Figure 15

Magnesium Oxide Coated Gallium Arsenide Strip
Average resistance ~500 Megohms

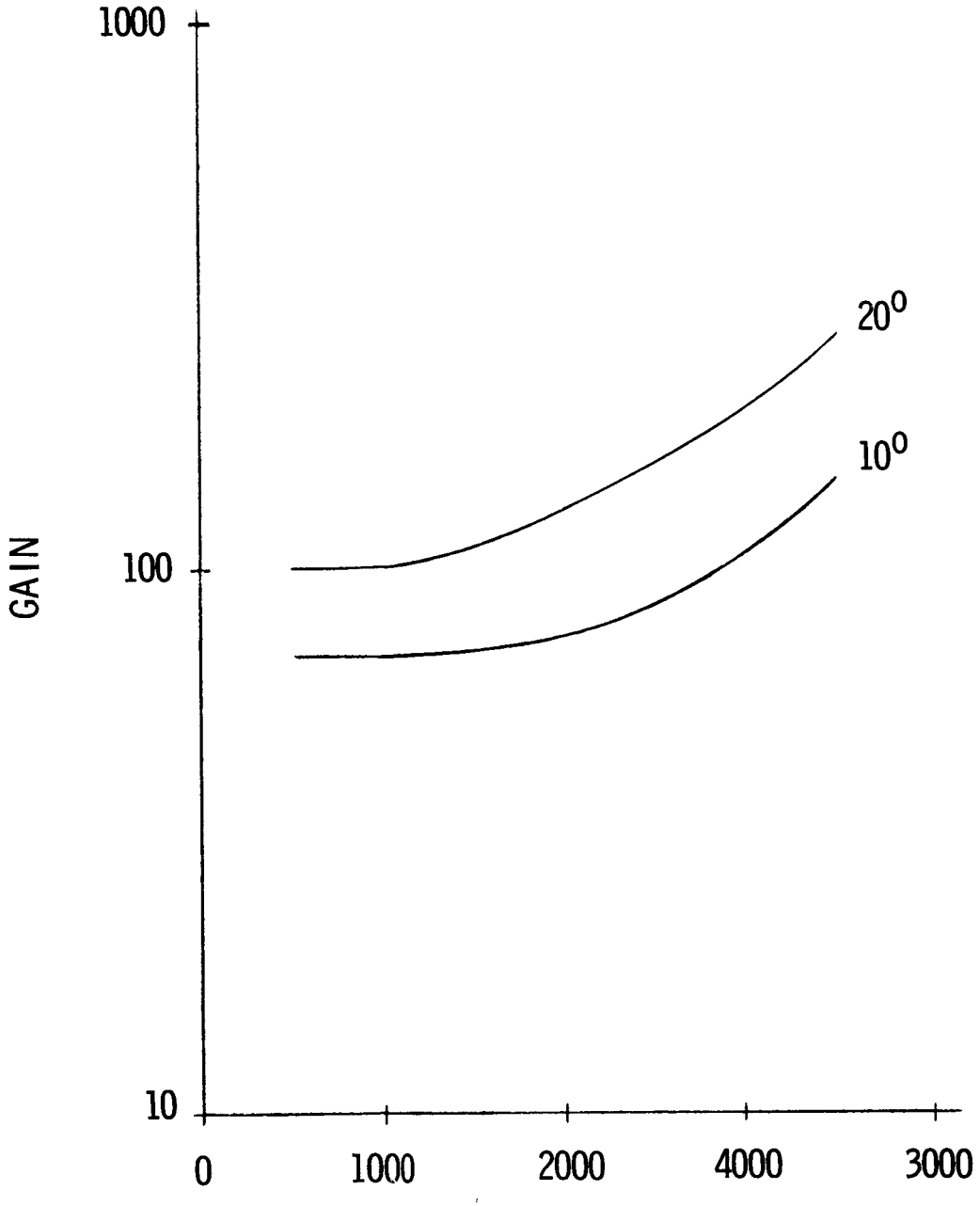

Multiplier Strip Gain vs. Applied Voltage

Figure 16

CBS LABORATORIES

Contract No. 950508

ADDENDUM TO FINAL REPORT

SHORT WIDE ANGLE, 1-1/2 INCH ELECTROSTATIC IMAGE DISSECTOR WITH PARALLEL PLATE RESISTIVE STRIP ELECTRONIC MULTIPLIER

Period Covered: February 22 1963 to November 1, 1965

Project No.: 5237

Date: March 2, 1966

Prepared For: Jet Propulsion Laboratory
California Institute of Technology
Pasadena, California

Prepared By: Jerry J. Karpinski
J. Karpinski
Tube Engineer

Approved By: Charles E. F. Misso
C.E.F. Misso, Section Head,
Electron Physics Department
CBS Laboratories, A Division
of Columbia Broadcasting System,
Inc., Stamford, Connecticut

Contract No. 950508

"This work was performed for the Jet Propulsion Laboratory, California Institute of Technology, pursuant to a sub-contract issued under Prime Contract NAS7-100 between the California Institute of Technology and the United States of America represented by the National Aeronautices and Space Administration."

4. FACEPLATE PROCESSING

Slight bowing of the faceplates was observed on some tubes made during this program. Investigation revealed that the plates were being heated beyond their annealing temperature during the application of the electrically conducting coating to the outer surfaces of the plates. Closer control of the processing temperature, which has to be very near the annealing point of the glass corrected this problem.

5.5 MAXIMUM RATING MULTIPLIER VOLTAGE

The dark current of five image dissectors was measured with their electron multipliers operating at 125 volts/stage and 150 volts/stage. The dark current of the tubes under these conditions is shown below.

ELECTRON MULTIPLIER INTERSTAGE VOLTAGE

Tube #	125 volts/stage Dark Current Microamperes	150 volts/stage Dark Current Microamperes	Increase in Dark Current Factor
M1294	.046	.24	5.2
M1300	.0065	.014	2.15
M1290	.06	.3	5.0
M1305	.02	.1	5.0
M1289	.05	.25	5.0

The above data suggests that a maximum factor of 5.5 would be a realistic specification for the increase in dark current resulting from increasing the electron multiplier interstage voltage from 125 volts to 150 volts.

If a factor of 5 is the maximum that can be tolerated the maximum operating voltage should be set at 145 volts per stage.

5.6 IMAGE SECTION VOLTAGE

Tests were conducted to determine the effect of increasing the image section voltage on the signal to dark current ratio.

Table II shows the signal to dark current ratio for image section voltage of 700, 1000 and 1500 volts respectively.

A negligible reduction in signal current occurred when the image section voltage was increased from 700 to 1000 volts, however, further

increases resulted in a reduction of signal. The reduction amounted to between 30 and 55% at 1500 volts. This was anticipated since a fall in the secondary emissive yield from the first dynode was expected with the increasing primary electron energy.

The increase in dark current varied considerably from tube to tube. It can be seen from the table that,in general, the increase was much greater in the more sensitive tubes. This is to be expected since these would more readily detect spurious conditions generated by the increased image section voltage. It should be noted that the signal current to dark current ratio of the two less sensitive tubes at 700 volts was almost exactly the same as that at 1000 volts.

Because of the great differences in gain and therefore the overall sensitivities at specified electron multiplier voltages it is not practical to establish a signal current to dark current ratio for various image section voltages. A more practical way would be to measure the signal to dark current ratio, for various image section voltages, at specified overall sensitivity levels. For example as dark current is specified in Paragraph 3.4.9 in JPL Specification GM050391-D5N. It is recommended that this be studied further since the data on tubes with similar apertures is limited.

TABLE II

SIGNAL CURRENT TO DARK CURRENT RATIO

Image Section	700 volts			1000 volts			500 volts		
Electron Multiplier Volts/Stage	105 volts			105 volts			105 volts		
Tube	Is	I_{DC}	Ratio	Is	I_{DC}	Ratio	Is	I_{DC}	Ratio
M1289	20	.014	1430	20	.054	370	15.5	6.4	2.42
M1290	2.35	.028	84	2.35	0.1	23.5	1.0	1.9	0.526
M1294	1.05	.052	202	1.05	.054	19.4	.76	.058	13.2
M1300	.96	.0034	282	.98	.0034	288	.65	.0038	.172
M1305	1.8	.0068	265	1.8	.018	100	1.5	3.5	.43

Electron Multiplier Volts/stage	135 volts			135 volts			135 volts		
M1289	230	.1	2300	230	.28	822	200	60.0	33.3
M1290	18	.27	665	18	.58	31.0	11.0	16.0	.69
M1294	10.5	0.5	.21	10.5	0.5	21	7	0.5	14
M1300	14.0	.0066	2120	14.0	.0066	2120	9	.06	150
M1305	21	.038	540	18	.058	310	10.5	35	.30

TUBE GAIN (ELECTRON MULTIPLIER VOLTAGE = 125 Volts/Stage)

M1289	M1290	M1294	M1300	M1305
2×10^{8}	5.9×10^{7}	4.7×10^{7}	6.9×10^{6}	9.7×10^{7}

5.7 PHOTOCATHODE FATIGUE

The effect of exposing bi-alkali and S-11 photocathodes to an illumination level of 2500 foot candles was studied.

Initially, various size areas of bi-alkali photocathodes in photomultipliers were exposed to three levels of illumination for one minute. The photocurrents from the respective areas before and one hour after the test exposure are shown in Table III below.

TABLE III

BI-ALKALI PHOTOCATHODES (PHOTOMULTIPLIERS)

Diameter of Cathode Area Exposed	Test Illumination 500 Ft.-Candles Photocurrent* Microamperes		Change %	1500 Ft.-Candles Photocurrent* Microamperes		Change %	2500 Ft-Candles Photocurrent* Microamperes		Change %
.9	.242	.242	0	1.425	1.475	+3.5	.2475	.255	+3
.4	.0405	.040	-1	.041	.041	0	.035	.0375	+2
.3	.026	.0263	-1	.026	.0262	+1	.01575	.0165	+4.8

* Measurements made at low light levels in test equipment.

Since the changes in photocurrent were very small and in the order of instrument and experimental error subsequent tests were made at one illumination level, 2500 foot candles. In addition, photoemission currents were monitored during the test exposure in order to get a more accurate indication of changes in photocathode sensitivity. The data in Table IV for S-11 photocathodes shows that the sensitivity of the photomultiplier cathode increased when they were exposed to the 2500 foot-candle illumination whereas

the sensitivity of the image dissectors photocathode fell by somewhat smaller amounts.

The spread in data suggests that the development of a pre-conditioning or aging process, for use at the end of the manufacturing processes, would be advantageous.

It is recommended that further tests should be conducted with photomultipliers made under more stringent controls and with additional image dissectors, in order to establish meaningful fatigue specifications. Comprehensive tests will be made with bi-alkali image dissectors made under JPL Contract No. 950784 when a series of thermal tests are completed.

TABLE IV

S-11 PHOTOCATHODE FATIGUE TESTS*

Tube #	Dia. of Cathode Areas Exposed	Photocurrent Microamperes		
		START	FINISH	CHANGE %
2159	.4	42	60	+43
4051	.4	32	44	+37
2456	.4	32	37	+16
2159	.3	22	26	+18
4051	.3	13	21	+61
2159	.9	180	240	+33
4051	.9	150	220	+47
2456	.9	200	270	+35
7866	.9	52	53.5	+3
		Image Dissectors		
M1105	.4	41	36	-12
M1105	1	210	190	-9.5
M1109	.4	48	45	-6.3
M1109	1	260	260	0
M1119	.4	90	75	-16.5
M1119	.9	540	420	-22

*Cathodes illumination 2500 foot-candles for 1 minute
Photocurrent readings taken at beginning and end of exposure